ACS Infectious Diseases

pubs.acs.org/journal/aidcbc Article

Anti-HIV-1 Activity of pepRF1, a Proteolysis-Resistant CXCR4 Antagonist Derived from Dengue Virus Capsid Protein

Iris Cadima-Couto, Alexandra Tauzin, João M. Freire, Tiago N. Figueira, Rúben D. M. Silva, Clara Pérez-Peinado, Catarina Cunha-Santos, Inês Bártolo, Nuno Taveira, Lurdes Gano, João D. G. Correia, Joao Goncalves, Fabrizio Mammano,* David Andreu,* Miguel A. R. B. Castanho,* and Ana Salomé Veiga*

Cite This: *ACS Infect. Dis.* 2021, 7, 6−22 Read Online

ACCESS | Metrics & More | Article Recommendations | Supporting Information

ABSTRACT: There is an urgent need for the development of new anti-HIV drugs that can complement existing medicines to be used against resistant strains. Here, we report the anti-HIV-1 peptide pepRF1, a human serum-resistant peptide derived from the Dengue virus capsid protein. *In vitro*, pepRF1 shows a 50% inhibitory concentration of 1.5 nM with a potential therapeutic window higher than 53 000. This peptide is specific for CXCR4-tropic strains, preventing viral entry into target cells by binding to the viral coreceptor CXCR4, acting as an antagonist of this receptor. pepRF1 is more effective than T20, the only peptide-based HIV-1 entry inhibitor approved, and excels in inhibiting a HIV-1 strain resistant to T20. Potentially, pepRF1 can be used alone or in combination with other anti-HIV drugs. Furthermore, one can also envisage its use as a novel therapeutic strategy for other CXCR4-related diseases.

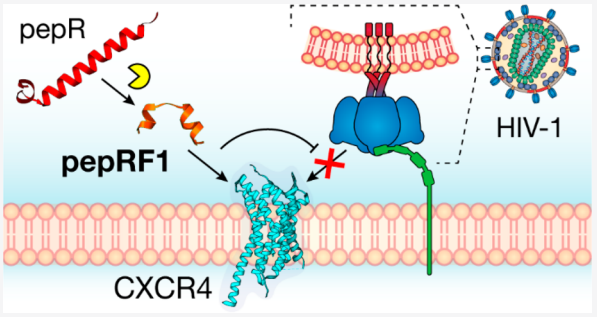

KEYWORDS: *HIV, antiviral drugs, peptide, CXCR4, antagonist*

Human immunodeficiency virus (HIV) is responsible for acquired immunodeficiency syndrome (AIDS), a condition characterized by $CD4^+$ T cell depletion and consequent susceptibility to opportunistic infections.[1] In 2019 there were 38 million people globally living with HIV, with nearly one-half of this population being treated with a combined antiretroviral therapy (cART).[2] cART, which generally consists of a triple drug regimen directed toward at least two distinct molecular targets, is broadly accepted as the most efficient way to control viremia.[3] However, this therapy does not lead to complete virus elimination, and the potential acquisition and transmission of HIV drug-resistant strains remains a therapeutic challenge.

The steady development of peptide-based drugs over the past decade is one of the most promising fields in drug discovery.[4,5] The specificity and high affinity of peptides toward their molecular targets is one of their main advantages, together with a low toxicity.[6] Several peptides have shown anti-HIV activity, targeting different steps of the HIV replication cycle such as fusion with the host cell,[7,8] reverse transcription,[9,10] integration,[11,12] and maturation.[13,14] T20 (enfuvirtide, Fuzeon) is emblematic of fusion inhibitor peptides used in the clinical management of HIV infection, preventing the merging of viral and cellular membranes, thus precluding virus entry.[15−17] HIV entry is a multistep process mediated by the viral envelope glycoprotein complex (Env), which consists of a trimer of heterodimers, each formed by a gp120 surface glycoprotein and a gp41 transmembrane protein.[18] Binding of gp120 to CD4 and to one of the chemokine receptors that serve as HIV coreceptor (CCR5 or CXCR4) triggers conformational changes, leading to the exposure of a hydrophobic peptide at the N-terminus of gp41, which inserts into the cellular membrane.[18] Then, two alpha helices (HR1 and HR2) on gp41 fold onto each other, forming a six-helix bundle for each Env trimer.[18] This rearrangement brings together the viral and cellular membranes, leading to their fusion.[18] T20, the only clinically approved fusion inhibitor, is a 36 amino acid HR2-derived sequence that, by binding to HR1, prevents the formation of the six-helix bundle.[15−17] T20 has been shown to suppress replication of HIV variants with multidrug resistance to reverse transcriptase and protease inhibitors.[16,17] However, its administration by high-dosage injection and its short *in vivo* half-life result in low efficacy and have limited its clinical application to "salvage" treatment.[19−21]

Received: December 19, 2019
Published: December 15, 2020

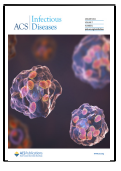

https://dx.doi.org/10.1021/acsinfecdis.9b00507
ACS Infect. Dis. 2021, 7, 6−22

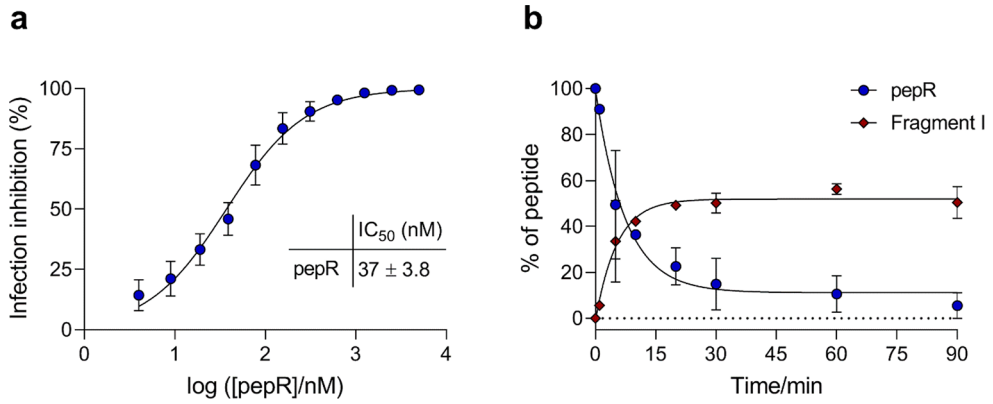

Figure 1. *In vitro* evaluation of pepR activity against HIV-$1_{NL4.3}$ and stability in serum. (a) Inhibition of viral infection was assessed against the laboratory-adapted strain HIV-$1_{NL4.3}$ (100 $TCID_{50}$) in the presence of increasing concentrations of pepR. Viral infectivity was quantified 48 h postinfection through luciferase reporter-enzyme activity and converted to percentage of viral infection inhibition. (b) Time course of pepR decay in human serum and of emerging main byproduct, Fragment I. pepR curve was fitted to an exponential decay for half-life ($t_{1/2}$) estimation.

Table 1. Fragments Resulting from pepR Digestion by Serum[a]

Peptide	Retention time (min)	Observed mass (Da)	Sequence	Calculated mass (Da)
pepR	10.0	4278	LKRWGTIKKSKAINVLRGFRKEIGRMLNILNRRRR	4279.20
Fragment I	6.4	2012	LKRWGTIKKSKAINVLR	2011.47
Fragment II	6.9	1925	RKEIGRMLNILNRRR KEIGRMLNILNRRRR	1925.32 1925.32
Fragment III	7.3	1856	LKRWGTIKKSKAINVL	1855.28
Fragment IV	7.7	2956	LKRWGTIKKSKAINVLRGFRKEIGR GTIKKSKAINVLRGFRKEIGRMLNIL KKSKAINVLRGFRKEIGRMLNILNR	2955.57 2956.62 2955.59
Fragment V	8.5	2216	LKRWGTIKKSKAINVLRGF GTIKKSKAINVLRGFRKEIG KSKAINVLRGFRKEIGRML	2215.70 2215.65 2216.71
Fragment VI	8.8	2285	RGFRKEIGRMLNILNRRR GFRKEIGRMLNILNRRRR	2285.73 2285.73

[a]Primary structures for peaks I to VI on Figure S1, proposed on the basis of MS data. MS spectra of the fragments are shown in Figure S2.

As with any antiretroviral, the emergence of T20-resistant viral variants has been observed both *in vitro*[19] and in the clinic.[22−25]

Antimicrobial peptides (AMPs) are a group of molecules known for their broad-spectrum activity against bacteria, fungi, and viruses. Despite the considerable number of AMPs described, and the fact that some have been shown to directly inhibit one or more steps in the HIV replication cycle,[26,27] in-depth studies of their anti-HIV potential are scarce. We have previously discovered a peptide,[28,29] pepR, that is derived from the Dengue virus capsid protein and displays antibacterial activity against both Gram-positive and -negative bacteria.[30] Here, we investigated the anti-HIV-1 activity of pepR and showed that the peptide is able to inhibit HIV-1 infection. Since one of the major limitations in the development of peptide-based drugs is their vulnerability to proteolytic degradation,[31] we searched for an active, human serum-resistant fragment of pepR. We discovered a resistant fragment, hereafter pepRF1, that shows remarkably potent activity against lab-adapted HIV-1 strains, patient-derived viruses, and a T20-resistant virus. Mechanistic studies on its anti-HIV-1 activity additionally show that pepRF1 is a potent CXCR4 antagonist that prevents CXCR4-tropic HIV-1 entry at nanomolar level, which demonstrate its potential as a drug lead.

RESULTS

pepR Anti-HIV-1 Activity and Serum Stability. The antiviral activity of pepR against the HIV-1 laboratory-adapted strain NL4.3 (HIV-$1_{NL4.3}$) was evaluated using a single-cycle infectivity assay. As shown in Figure 1a, pepR inhibited infection of TZM-bl cells with an IC_{50} of 37 nM.

The susceptibility of pepR to human serum was investigated by HPLC-MS. pepR underwent relatively fast decay (Figure 1b), with >90% of the initial product consumed after 90 min. A $t_{1/2}$ of 3.7 min was determined by fitting of an exponential function to experimental data. The HPLC profile of the digest (Figure S1) shows a main peak (Fragment I) reaching maximum intensity at ∼20 min incubation with serum and remaining constant henceforth. On the basis of MS data, a primary structure (LKRWGTIKKSKAINVLR, Table 1 and Figure S2) could be unequivocally proposed for Fragment I, which could plausibly result from trypsin-like cleavage of pepR at Arg^{17}-Gly^{18}. An alternative, more complex pathway would entail chymotrypsin-like cleavage at Phe^{19}-Arg^{20} to give intermediate LKRWGTIKKSKAINVLRGF (one among possible Fragment V candidates, Table 1), which would then

https://dx.doi.org/10.1021/acsinfecdis.9b00507
ACS Infect. Dis. 2021, 7, 6−22

Table 2. Fragment I (pepRF1), an Abridged Version of pepR

peptide	sequence	length (residues)	molecular mass (Da)	net charge
pepR	LKRWGTIKKSKAINVLRGFRKEIGRMLNILNRRRR-amide	35	4278.19	+13
pepRF1	LKRWGTIKKSKAINVLR-amide	17	2010.48	+7

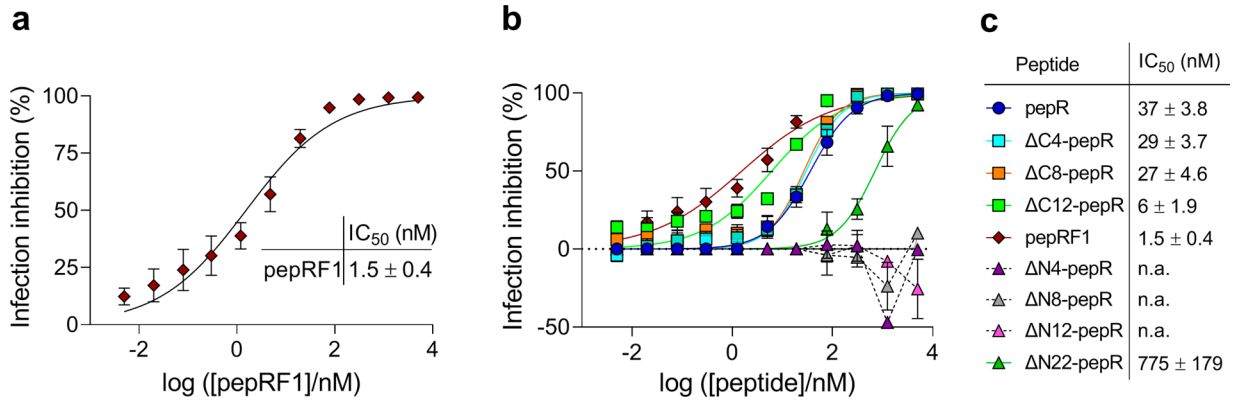

Figure 2. *In vitro* evaluation of peptides' activity against HIV-$1_{NL4.3}$ infection of TZM-bl cells. Inhibition of viral infection was assessed against the laboratory-adapted strain HIV-$1_{NL4.3}$ (100 $TCID_{50}$) in the presence of increasing concentrations of pepRF1 (a) and pepR derivatives (b). A sequence−activity relationship analysis of pepR derivatives was performed, and dose−response curves (b) and corresponding mean IC_{50} values (c) were compared to the ones obtained for pepR and pepRF1. In all assays, viral infectivity was quantified 48 h postinfection through luciferase reporter-enzyme activity and converted to percentage of viral infection inhibition.

Table 3. Designed Peptide Derivatives Obtained by Sequential Truncation of pepR

Peptide	Sequence	Length	Net charge
pepR	LKRWGTIKKSKAINVLRGFRKEIGRMLNILNRRRR	35	+13
ΔC4-pepR	LKRWGTIKKSKAINVLRGFRKEIGRMLNILN	31	+9
ΔC8-pepR	LKRWGTIKKSKAINVLRGFRKEIGRML	27	+9
ΔC12-pepR	LKRWGTIKKSKAINVLRGFRKEI	23	+8
ΔN4-pepR	GTIKKSKAINVLRGFRKEIGRMLNILNRRRR	31	+11
ΔN8-pepR	KSKAINVLRGFRKEIGRMLNILNRRRR	27	+10
ΔN12-pepR	INVLRGFRKEIGRMLNILNRRRR	23	+8
ΔN22-pepR	GRMLNILNRRRR	13	+6

undergo stepwise carboxypeptidase clipping of C-terminal Phe and Gly.

Aside from Fragment I, the other five peaks (II−VI) observed by HPLC (Figure S1) are of much lower intensity. For Fragment III, an unequivocal sequence can be assigned from MS data, while for Fragments II and IV−VI, two or more quasi-isobaric sequences can be proposed (Table 1), suggesting degradation pathways of minor importance compared to those leading to Fragment I accumulation. It was obvious at this point that, given its superior serum stability and predictable reduction in production costs, as a result of pepR > 50% size reduction, Fragment I (henceforth pepRF1) should be explored as an alternative antiviral candidate over pepR. Accordingly, a synthetic replica (in C-terminal carboxamide version) was also prepared and evaluated (Table 2).

pepRF1 Anti-HIV Activity and Toxicity. The antiviral activity of pepRF1 against HIV-$1_{NL4.3}$ was assessed, and the IC_{50} value obtained, 1.5 nM, revealed it as even more potent than its parent pepR, on the inhibition of infection of TZM-bl cells (Figure 2a).

In fact, a sequence−activity relationship analysis revealed that the domain responsible for the antiviral activity of pepR is located in the N-terminal region that includes pepRF1 sequence. pepR analogues obtained by stepwise residue deletions at both N- and C-termini (Table 3) were tested against HIV-$1_{NL4.3}$. The results, Figure 2b, clearly show that the sequential deletion of amino acid residues toward the N-terminal region of the peptide resulted in an increase of the anti-HIV-1 activity: IC_{50} = 29 nM for ΔC4-pepR, IC_{50} = 27 nM for ΔC8-pepR, and IC_{50} = 6 nM for ΔC12-pepR. These results are in agreement with the IC_{50} value of 1.5 nM obtained for pepRF1, which would correspond to ΔC18-pepR. On the other hand, the peptides generated by the sequential deletion of amino acid residues at the N-terminal region (ΔN4-, ΔN8-, ΔN12-pepR) turned out to be inactive against HIV-$1_{NL4.3}$.

Importantly, pepRF1 has no cytotoxic effects on TZM-bl cells (Figure S3a), which shows that the antiviral effect is not due to toxicity caused by the peptide. Additionally, pepRF1 has no cytotoxic effects on $CD4^+$ T-lymphocytes and peripheral blood mononuclear cells (PBMCs) for concentrations up to 80 μM (Figure S3b,c), the highest concentration tested, corresponding to a potential therapeutic window of >53 000. To further test the potential toxicity of the peptide, an *in vivo* Maximum Tolerated Dose (MTD) assay was performed in mice. Two doses, 3 and 10 mg/kg were tolerated without causing any significant body weight changes or mortality. At 30 mg/kg, pepRF1 caused the death of all tested mice within 15 min after intravenous (IV) administration. No significant abnormality was observed under gross necropsy. An MTD

https://dx.doi.org/10.1021/acsinfecdis.9b00507
ACS Infect. Dis. 2021, 7, 6−22

Table 4. Biodistribution Study of pepRF1^{67}Ga-NODA-GA in CD1 Mice at 15 min, 1, 4, and 24 h Postinjection[a]

	% ID/g ± SD			
tissue/organ	15 min	1 h	4 h	24 h
blood	3.8 ± 1.1	0.44 ± 0.04	0.11 ± 0.05	0.06 ± 0.04
liver	7.4 ± 1.4	6.4 ± 1.3	4.6 ± 0.8	1.6 ± 0.2
intestine	0.66 ± 0.06	0.7 ± 0.2	1.8 ± 0.8	0.04 ± 0.02
spleen	1.4 ± 0.1	0.6 ± 0.1	0.37 ± 0.06	0.12 ± 0.01
heart	1.15 ± 0.07	0.23 ± 0.01	0.10 ± 0.01	0.03 ± 0.00
lung	2.0 ± 0.3	0.37 ± 0.06	0.15 ± 0.03	0.05 ± 0.01
kidney	78.8 ± 10.5	69.4 ± 11.3	57.4 ± 4.3	11.6 ± 4.2
muscle	1.34 ± 0.02	0.20 ± 0.02	0.5 ± 0.1	0.04 ± 0.01
bone	2.6 ± 0.3	1.0 ± 0.1	0.08 ± 0.02	0.13 ± 0.01
stomach	1.1 ± 0.2	0.26 ± 0.05	0.12 ± 0.03	0.03 ± 0.02
pancreas	0.9 ± 0.1	0.20 ± 0.04	0.10 ± 0.01	0.03
brain	0.19 ± 0.07	0.03 ± 0.01	0.01 ± 0.00	0.00
excretion (% ID)	19.1 ± 0.7	45.1 ± 2.9	61.8 ± 1.7	90.0 ± 2.6

[a]Results are expressed as the average of percentage of injected dose (ID) per gram of tissue (% ID/g tissue; mean ± SD), n = 3.

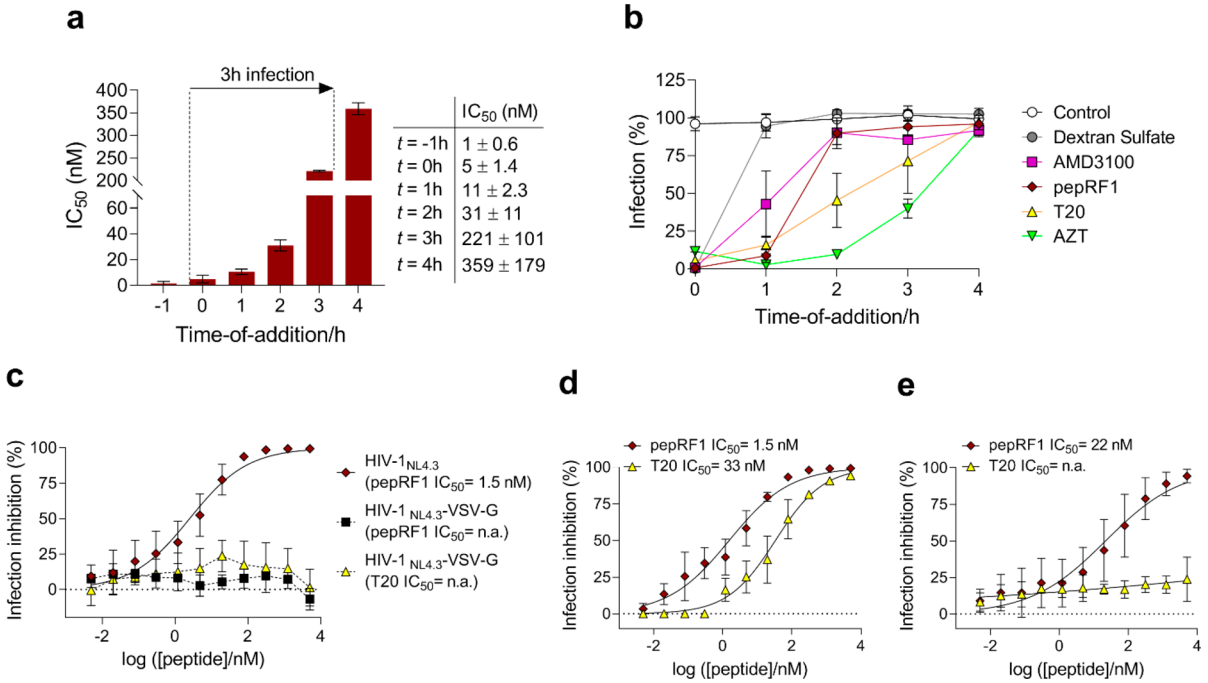

Figure 3. *In vitro* evaluation of pepRF1 time-of-addition and efficacy against HIV-$1_{NL4.3}$ entry into TZM-bl cells. (a) IC_{50} values were determined for pepRF1 by treating cells with increasing concentrations of each peptide at −1, 0, +1, +2, +3, or +4 h relatively to the moment of HIV-$1_{NL4.3}$ addition (100 $TCID_{50}$). IC_{50} values represent mean values obtained from three independent experiments. (b) Anti-HIV-1 activity of pepRF1 overtime relative to reference anti-HIV inhibitors. HIV-$1_{NL4.3}$ (100 $TCID_{50}$) was incubated with cells for 1 h and unbound virus was subsequently removed by repeated washing to synchronize infection. Cells were treated with 1 μM of pepRF1 and reference inhibitors (dextran sulfate, AMD3100, T20, and AZT) at 0, +1, +2, +3, or +4 h relatively to the moment of virus addition. The percentage of infection was taken relatively to the control (viruses in the absence of inhibitors). (c) The antiviral activity of pepRF1 against HIV-$1_{NL4.3}$-VSV-G was determined by infecting TZM-bl cells in the presence of increasing concentrations of the peptide. T20, which targets HIV-1 gp41, was tested against HIV-$1_{NL4.3}$-VSV-G, as a control. (d,e) The effect of pepRF1 on the target cell was studied by preincubating cells for 1 h with increasing concentrations of pepRF1 or T20 (control). After incubation, HIV-$1_{NL4.3}$ (100 $TCID_{50}$) was added to cells and infection was allowed for proceed for 3 h in the presence of peptides (d). Alternatively, cells were washed to remove peptides, HIV-$1_{NL4.3}$ (100 $TCID_{50}$) was added to cells, and infection was allowed to proceed for 3 h in the absence of peptides (e). In all assays, viral infectivity was quantified 48 h postinfection through luciferase reporter-enzyme activity and converted to percentage of viral infection inhibition.

dose of 10 mg/kg of pepRF1 through IV injection was thus established, corresponding to an initial concentration of 43 μM in an average blood volume in mice of 2.5 mL, before metabolism and plasma-protein binding effects. Although the *in vitro*−*in vivo* correlation is only approximate, the 43 μM MTD value is 4 orders of magnitude higher than the concentration (1.5 nM) needed to inhibit 50% of infection, which underlines the low toxicity of the peptide. Consistent with these results, *in vivo* biodistribution evaluated at four time points (15 min, 1, 4, and 24 h) after IV administration of the radiolabeled conjugate pepRF1^{67}Ga-NODA-GA to CD1 mice, shows a fast blood clearance and no accumulation of radioactivity in any organ, except in the excretory organs, particularly the kidneys, which is most likely related to renal

https://dx.doi.org/10.1021/acsinfecdis.9b00507
ACS Infect. Dis. 2021, 7, 6−22

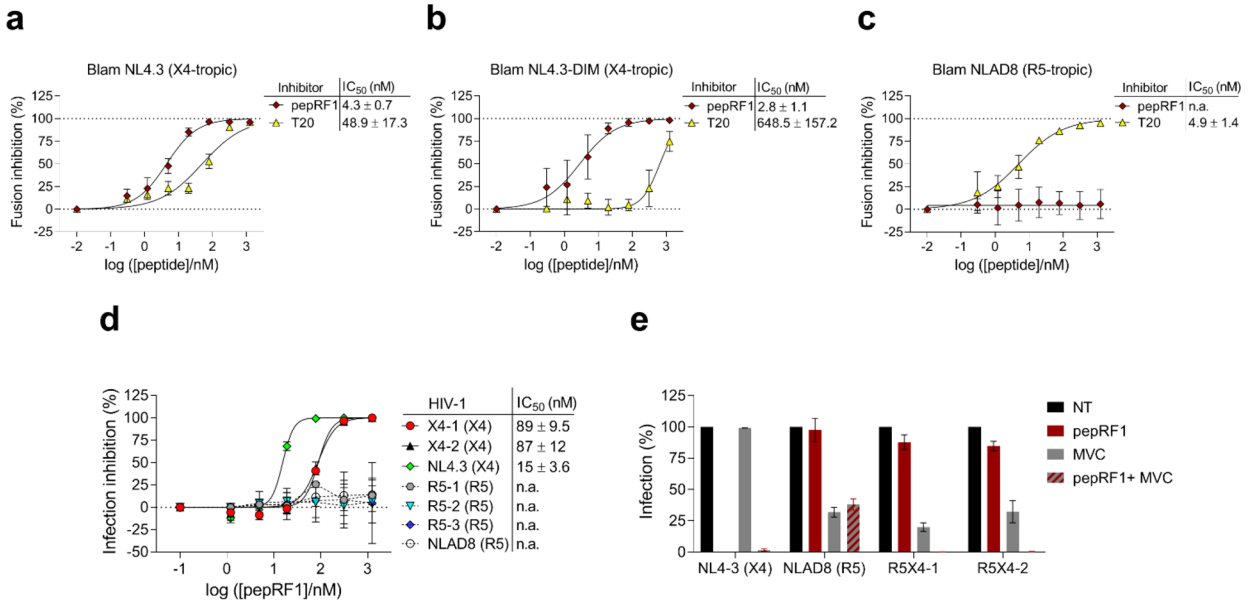

Figure 4. Inhibition by pepRF1 of viruses with different coreceptor usage. A virus-cell fusion assay based on the use of virions containing the β-lactamase-Vpr chimeric protein was performed using the CXCR4-tropic HIV-1 strains Blam NL4.3 (a) and Blam NL4.3-DIM (T20-resistant) (b), and the CCR5-tropic HIV-1 strain Blam NLAD8 (c). MT4R5 cells treated with increasing concentrations of pepRF1, pepR or T20 (control) were exposed to the different HIV-1 strains. Viral fusion and its inhibition was quantified by measuring the percentage of cells in which a fluorescent substrate of β-lactamase (CCF2) was cleaved, as compared to untreated controls. (d) Dose−response curves, and corresponding mean IC_{50} values for inhibition of viral infection of pepRF1 against viruses carrying primary CXCR4-tropic envelopes (clones X4−1 and X4−2) and CCR5-tropic envelopes (clones R5−1, R5−2 and R5−3) isolated from a patient, and against the reference strains NL4.3 (CXCR4-tropic) and NLAD8 (CCR5-tropic). Infection inhibition was evaluated by infecting TZM-bl cells in the presence of increasing concentrations of pepRF1. Viral infectivity was measured 40 h postinfection through β-galactosidase reporter-gene expression and converted to percentage of viral infection inhibition. Data points represent the average of results obtained from two independent experiments. (e) Inhibition of viruses carrying patient derived dual-tropic Env complexes (R5X4−1 and R5X4−2) by MVC, pepRF1, and MVC+pepRF1. TZM-bl cells were treated with a single concentration of each molecule before being exposed to the viruses, and the extent of infection was measured as in (d).

reabsorption of radiopeptide metabolites. Importantly, the excretion rate is in line with what is described for other peptides[32,33] cleared through renal pathways (Table 4). Additional work is needed to optimize the pharmacokinetics and blood distribution of the peptide for translational uses.

pepRF1 Targets an Early Step in HIV-1 Entry. The HIV replication cycle consist of different stages that occur in a well-established chronological order.[34] Time-of-addition (TOA) experiments are a commonly used approach to study the mode of action of HIV inhibitors,[35] namely which replication step is being targeted. First, we determined if pepRF1 targets HIV-1 before, during, or after viral entry into cells. pepRF1 was incubated with HIV-$1_{NL4.3}$ before addition to cells ($t = -1$ h), added to cells at different time-points during infection ($t = 0$, 1, 2 h), or added to cells after infection ($t = 3$, 4 h). The inhibitory effect of pepRF1 was only observed when the peptide was added before or during, but not after the virus infection period, indicating that it acts during viral entry into cells (Figure 3a). This effect was more pronounced when pepRF1 was preincubated with virions ($t = -1$ h) (IC_{50} = 1.2 nM), or added to the cells together with virions ($t = 0$ h) (IC_{50} = 2.5 nM), suggesting that the peptide targets an early event during viral entry. The results also showed that pepRF1 was more potent than pepR at inhibiting HIV-1 infection at all the time-points tested (Figure S4).

To better discriminate which step(s) of HIV-1 replication are inhibited by pepRF1, we studied its activity against HIV-$1_{NL4.3}$ over time relative to reference drugs.[35] HIV-$1_{NL4.3}$ virions were added to cells and incubated for 1 h at 37 °C. pepRF1 and the well-characterized inhibitors dextran sulfate, AMD3100, T20, and zidovudine (AZT) were added to cells together with HIV-$1_{NL4.3}$ virions ($t = 0$ h), or at different time-points during the early phase of the virus replication cycle (t = 1, 2, 3, 4 h). As expected, dextran sulfate, an inhibitor of viral adsorption to the host cell,[35,36] became ineffective if added 1 h after infection. In this case the calculated time-of-drug-addition that maintains 50% inhibition (t_{50}) was 0.8 h (t_{50} = 0.8 h) (Figure 3b). The bicyclam AMD3100, a CXCR4 antagonist that prevents HIV-1 attachment to the coreceptor,[37−39] became ineffective soon after infection (t_{50} = 1.4 h for AMD3100). The viral fusion inhibitor T20 remained effective up to a slightly later time (t_{50} = 1.8 h), which is consistent with its inhibition of the fusion event, occurring after receptor binding.[15−17] Finally, AZT blocked HIV-1 replication even if added with significant delay (t_{50} = 3.1 h), which is in accordance with its intracellular targeting of the reverse transcription process.[35,40] pepRF1 inhibited infection with a t_{50} of 1.3 h, similar to AMD3100. This suggests that pepRF1 blocked HIV entry into cells by interfering with a process in between virus adsorption and fusion, possibly by blocking attachment of viral glycoproteins to cell receptors.

To test this hypothesis, a viral inhibition assay was performed using HIV-1 virions pseudotyped with the envelope glycoprotein G from the vesicular stomatitis virus (VSV-G), HIV-$1_{NL4.3}$-VSV-G. This modified virus enters the cells via endocytosis and later fusion within acidified endosomes, without the requirement for HIV glycoproteins (gp120 and gp41) and cell membrane HIV receptor (CD4) and coreceptors (CCR5 and CXCR4). As shown in Figure 3c, pepRF1 was not able to inhibit infection of HIV-$1_{NL4.3}$-VSV-G.

https://dx.doi.org/10.1021/acsinfecdis.9b00507
ACS Infect. Dis. 2021, 7, 6−22

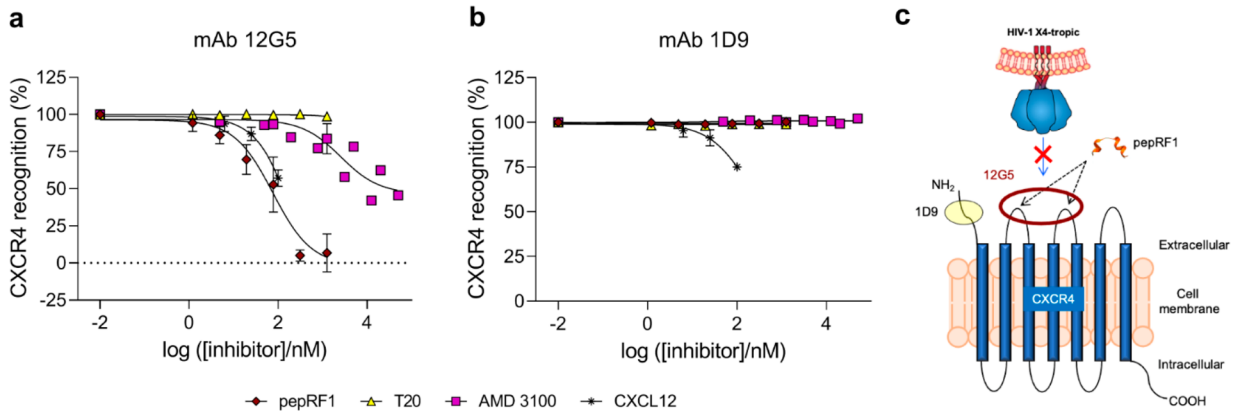

Figure 5. Effect of pepRF1 on CXCR4 recognition at cell surface. Primary $CD4^+$ T-lymphocytes were preincubated for 90 min with pepRF1 at 37 °C. The cells were then stained with the mAb 12G5 (a) or 1D9 (b), and analyzed by flow cytometry. T20, AMD3100 and CXCL12 were used as controls. The results are expressed as percent of cells positive for the surface expression of CXCR4, as compared to untreated controls. (c) mAbs 1D9 and 12G5 have distinct binding sites on CXCR4. As the presence of pepRF1 reduced the recognition of CXCR4 by 12G5 but not 1D9, the binding site of pepRF1 may either occupy or perturb the conformation of the first and/or second extracellular loops of the coreceptor.

The same was observed for pepR (Figure S5) and T20. This clearly shows that viral inhibition by pepRF1 targets the HIV Env-mediated entry process.

pepRF1 Inhibits HIV-1 Entry by Targeting the Host Cell. HIV-1 entry is a multistep process that progresses through viral gp120 binding to CD4 cell receptor, coreceptor engagement (CCR5 or CXCR4), and fusion with the host cell membrane.[18] Several peptides have been shown to block HIV infection by interfering with any of these steps in the viral entry process.[7−14,27] The above results showed that pepRF1 blocks HIV-1 entry into the host cell but the specific molecular target of this drug remained elusive. To investigate if pepRF1 targets the virion, the cell, or both, TZM-bl cells were preincubated with increasing concentrations of the peptide. T20 was used as a control since it is known to target the viral gp41. After incubation, HIV-$1_{NL4.3}$ was added to cells and infection was allowed to proceed for 3 h in the presence of pepRF1 or T20. In a different set of experiments, after preincubation with the peptides, cells were washed to remove the peptides, and HIV-$1_{NL4.3}$ was added to cells for 3 h. As shown in Figure 3d, both pepRF1 and T20 were able to inhibit infection by HIV-$1_{NL4.3}$ when present at the time that viruses were added to the cells. However, when the viruses were added after washing the cells for peptide removal, the ability of T20 to inhibit infection was completely abrogated (Figure 3e). This was expected because exposure of T20 target (the HR1 domain in gp41) only takes place after the virus has interacted with its receptors. On the other hand, pepRF1 was able to inhibit infection in spite of cell washing. This shows that during the incubation period with cells, the peptide was able to establish a durable interaction with a cellular component.

To further exclude a possible direct action of pepRF1 at the level of the viral membrane, the impact of pepRF1 on HIV-1 structural integrity was studied and the result showed that the peptide does not cause viral particle disruption (Figure S6).

pepRF1 Inhibits HIV-1 Cell Entry in a Coreceptor Specific Manner. The above results show that pepRF1 specifically inhibits HIV entry (Figure 3) by interacting with a cellular factor (Figure 3d,e). To study the target used by pepRF1 to block HIV-1 entry, a direct virus-cell fusion assay was performed based on the incorporation of Vpr-β-lactamase chimeric proteins (Vpr-Blam) into HIV-1 virions and their subsequent delivery into the cytoplasm of target cells as a result of virion fusion. This transfer was then detected by enzymatic cleavage of the CCF2 dye, a fluorescent substrate of β-lactamase (Blam), loaded into the target cells. This is the validated assay to assess the extent and the kinetics of HIV-1 fusion with target cells.[41,42] HIV-1 reporter pseudoviruses bearing the Vpr-β-lactamase chimera (Vpr-Blam) with CXCR4-tropic envelopes (Blam NL4.3 or Blam NL4.3-DIM)[43] were produced and used to infect MT4R5 cells in the absence and in the presence of increasing concentrations of pepRF1. The ability of pepRF1 to inhibit viral fusion was compared to pepR and T20. The results showed that pepRF1 was the most efficient inhibitor of Blam NL4.3 (IC_{50} = 4.3 nM) as compared to T20 (IC_{50} = 48.9 nM) (Figure 4a) and pepR (IC_{50} = 32.9 nM) (Figure S7). In addition, pepRF1 was able to inhibit Blam NL4.3-DIM, resistant to T20, with an IC_{50} of 2.8 nM (Figure 4b). Interestingly, in contrast to T20, neither pepRF1 nor pepR were able to inhibit infection by the CCR5-tropic virus, Blam NLAd8 (Figure 4c and Figure S7), showing specificity toward CXCR4-tropic viral strains.

pepRF1 Inhibits CXCR4-Tropic HIV-1 Carrying Patient-Derived Envelope Glycoproteins. We also investigated the ability of pepRF1 to inhibit infection of five different HIV-1 molecular clones carrying primary CXCR4 or CCR5-specific HIV-1 envelope glycoproteins. These strains carry gp120 and the extracellular part of gp41 issued from variants present in two patients, as described elsewhere.[44] As shown in Figure 4d, pepRF1 potently inhibited the two patient-derived CXCR4-tropic viruses, X4−1 and X4−2, in addition to the CXCR4 reference strain used in the previous assays (HIV-$1_{NL4.3}$). In contrast, it was not able to inhibit the three CCR5-tropic viruses, R5−1, R5−2, and R5−3, and the CCR5 reference strain (NLAD8). The same was observed for pepR (Figure S7). These results clearly reinforce the specificity of pepRF1 toward CXCR4-tropic HIV strains.

In addition to pure CCR5-tropic or CXCR4-tropic viruses, some variants are able to use both CCR5 and CXCR4 (in addition to CD4) to enter target cells.[45] These dual-tropic (or R5X4) viral variants may display differential efficacy in the use of the two coreceptors, and inhibition of both pathways is necessary to preclude virus infection. We thus tested the susceptibility of two patient-derived dual-tropic viruses to inhibition by pepRF1 alone and in combination with the CCR5 specific inhibitor maraviroc (MVC).[46] In parallel, we

https://dx.doi.org/10.1021/acsinfecdis.9b00507
ACS Infect. Dis. 2021, 7, 6−22

tested under the same conditions the two reference strains HIV-$1_{NL4.3}$ and NLAD8 (Figure 4e). The two viruses carrying patient-derived dual-tropic Env glycoproteins (R5X4−1 and R5X4−2) were partially inhibited by the CCR5 inhibitor MVC, and not significantly inhibited by pepRF1 at the dose used here; however, the addition of pepRF1 to MVC resulted in full-inhibition of virus infection, consistent with the requirement of occupation of both coreceptors for dual-tropic virus inhibition. As expected, pepRF1 was sufficient to inhibit HIV-$1_{NL4.3}$, while at dose used here MVC only partially inhibited NLAD8, but in this case the addition of pepRF1 had no additional effect. Similar results were obtained with pepR (Figure S7).

pepRF1 Prevents Viral Fusion without Inducing CXCR4 Internalization. On the basis of the above observations, the most likely target of pepRF1 appeared to be the coreceptor CXCR4. To unravel the mechanism underlying peptide action, the effect of pepRF1 on CXCR4 recognition at the surface of the cell membrane was studied by flow cytometry on primary $CD4^+$ T-lymphocytes. T20,[15−17] AMD3100,[37−39] and the chemokine CXCL12 (C-X-C motif ligand 12), the natural ligand of CXCR4, also known as SDF-1 (stromal cell-derived factor 1),[47,48] were used as controls. To determine whether pepRF1 interact directly with CXCR4, we first used mAb 12G5, which is directed against a bridging epitope spanning the first and second extracellular loops of CXCR4.[38,49] As shown in Figure 5a, CXCR4 detection at the surface of the cell was reduced in a dose dependent fashion, to undetectable levels, in the presence of both pepRF1 and pepR (Figure S8). The same was observed for AMD3100, in accordance with previous studies.[38,49] As expected, T20 had no effect on CXCR4 detection. These results suggest that pepRF1 and pepR interact directly with CXCR4, inhibiting CXCR4-epitope recognition by mAb 12G5, which could ensue by competitive binding, by changing the conformation of the coreceptor, or by inducing its internalization.

We next explored if the loss of CXCR4 detection from the surface of the cell was due to coreceptor internalization rather than competitive binding or conformational change. A different antibody, 1D9, that targets the N-terminal domain of CXCR4,[49] was used. The binding of this mAb will not be perturbed by changes in the conformation of the coreceptor at the ligand binding site.[49,50] In this way, loss of detection of 1D9 from the surface of the cells would be strongly indicative of CXCR4 internalization. As shown in Figure 5, 1D9 binds equally well to CXCR4 in the presence and absence of pepRF1 and pepR (Figure S8), showing that the coreceptor is still on the cell surface, but is occupied/modified by the peptides, which prevented 12G5 binding. The same was observed for AMD3100, which does not induce CXCR4 internalization.[51] The same experiments were performed using CXCL12, which upon interaction with the coreceptor induces its internalization and activates a complex cascade of intracellular signaling pathways.[38,39,47−49,51] At the surface level, pepRF1, pepR, AMD3100, and CXCL12, reduced the recognition of CXCR4 by 12G5 (Figure 5a). In contrast, only CXCL12 decreased recognition of CXCR4 by mAb 1D9 (Figure 5b), as described in previous studies.[49]

To exclude a possible effect of pepRF1 and pepR on CCR5 recognition on the surface of cells, primary cells were also labeled with an anti-CCR5 antibody. Results show that the recognition was unaffected by pepRF1, pepR, AMD3100, and T20 (Figure S9), in agreement with the infection data showing an effect only on CXCR4-mediated HIV entry. Overall the data show that pepRF1 binds to CXCR4 coreceptor, in a binding site that occupy or perturb the conformation of the first and/or second extracellular loops, preventing its use by HIV, but without inducing its internalization (Figure 5c).

pepRF1 Is an Antagonist of CXCR4. The transient increase in cytosolic Ca^{2+} concentration is an essential signaling pathway that is activated upon CXCR4 stimulation.[38,39,47−49,51] The binding of the natural ligand, CXCL12, to CXCR4 elicits a transient increase in intracellular Ca^{2+} concentration, classifying the ligand as a CXCR4 agonist.[38,39,47−49,51] On the other hand, the compound AMD3100 by itself does not induce intracellular Ca^{2+} signaling and when both are present, AMD3100 antagonizes the action of CXCL12.[38,39,47−49,51] For this reason, AMD3100 has been defined as a pure and specific CXCR4 antagonist.[38,39,47−49,51] In this study, we used a cell-based fluorescence assay to measure intracellular Ca^{2+} levels and determined the agonist or antagonist nature of pepRF1 and pepR. CXCL12 and AMD3100 were used as controls. THP-1 monocytes were first loaded with the fluorescent Ca^{2+} indicator Fluo-4 AM and incubated for 1 h. The agonist or antagonist effect of the compounds on the intracellular Ca^{2+} influx was then determined by adding the compounds to cells (alone or in combination), followed by immediate detection of variations in cytosolic Ca^{2+} levels (Figure 6). Treatment of cells with

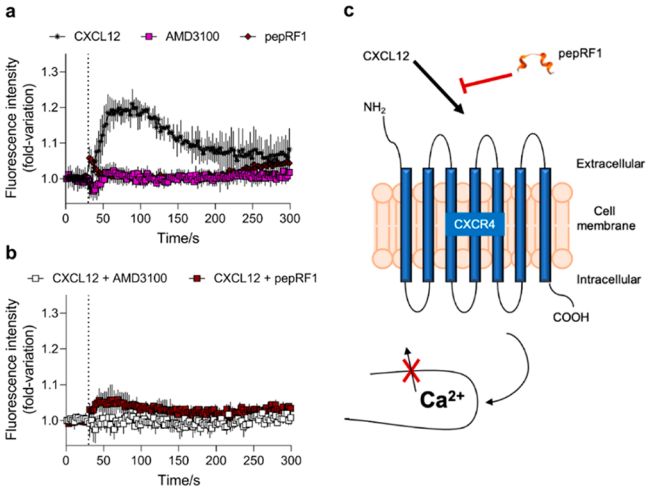

Figure 6. Impact of pepRF1 on CXCR4-associated Ca^{2+} intracellular mobilization. Time-resolved fluorescence emission intensity profiles of Fluo-4 within THP-1 cells upon treatment with pepRF1 (1.25 μM), AMD3100 (50 μM), and CXCL12 (50 nM), alone (a) or in combination (b). Fluo-4 basal fluorescence emission intensity was collected for 30 s prior to addition of individual compounds and combinations, and followed for an additional 270 s. A mark was added to the t horizontal axis, at 30 s, for clarity. Data was normalized to the basal Fluo-4 fluorescence emission intensity values, measured at t = 0 s. (c) pepRF1 was able to antagonize CXCL12 action, showing that it acts as CXCR4 antagonist by inhibiting the Ca^{2+} release from the endoplasmic reticulum.

CXCL12 alone elicited a transient increase in Ca^{2+} influx, which is in accordance with its expected agonist function.[38,39,47−49,51] In contrast, same as with AMD3100, pepRF1 had no effect on cytosolic Ca^{2+} levels (Figure 6a). Surprisingly, pepR showed strong agonistic activity that lasted for the entire duration of the assay (Figure S10). Like AMD3100, pepRF1 was able to antagonize CXCL12 action

https://dx.doi.org/10.1021/acsinfecdis.9b00507
ACS Infect. Dis. 2021, 7, 6−22

(Figure 6b), showing that it acts as CXCR4 antagonist (Figure 6c). Interestingly, when compared to AMD3100, pepRF1 was more efficient at counteracting the strong agonist activity of pepR (Figure S10).

DISCUSSION

In the present study, we have developed a new potent CXCR4-targeted inhibitor of HIV-1 entry, pepRF1, derived from the Dengue virus capsid protein. This highly stable peptide is the serum-resistant fraction of pepR, a peptide previously developed by us with antibacterial activity and cell-penetrating properties.[28−30] Remarkably, pepRF1 shows impressive anti-HIV-1 activity when compared to T20, the only peptide-based HIV-1 fusion inhibitor approved by FDA for clinical use. In addition, pepRF1 is able to inhibit a T20-resistant strain, HIV-$1_{NL4.3}$-DIM, at a low nanomolar concentration.

Our detailed studies on the mechanism of action reveal that pepRF1 inhibitory activity is specific for CXCR4-tropic HIV-1 strains, preventing viral entry into target cells by binding to CXCR4 coreceptor without inducing its internalization. If we hypothesize that pepRF1 inhibition of the CXCR4-epitope recognition by mAb 12G5 is due to competitive binding, it is reasonable to assume that its binding site is located on the first and/or second extracellular loops of the coreceptor. Additionally, given the peptide cationic nature, an electrostatic interaction might be involved on its binding to the coreceptor, as it has been shown to other peptides with affinity for CXCR4.[52,53] Like AMD3100, a small molecule inhibitor that strongly restricts CXCR4 HIV-1 infection, pepRF1 does not elicit intracellular Ca^{2+} influx indicating that the peptide does not act as a CXCR4 agonist.[37−39,47−49,51] Moreover, pepRF1, as opposed to pepR, potently inhibited the intracellular Ca^{2+} signaling elicited by the CXCR4 natural ligand CXCL12, acting as an antagonist. Despite these differences, both peptides are strong inhibitors of HIV-1 infection.

Inhibition of CXCR4 as a strategy to fight HIV-1 infection is important, because CXCR4-tropic HIV strains are considered to be more pathogenic than CCR5-tropic ones. Indeed, their appearance during an extended time course of infection correlates with a decline in the $CD4^+$ T-cell count leading to a more rapid progression to AIDS symptoms.[54] Furthermore, drug resistance is also more often linked to CXCR4-tropic strains,[55] posing an urgent need for the development of effective drugs that block CXCR4-mediated HIV infection. In such a scenario, the use of CXCR4 antagonists may be useful in delaying the onset of disease. On the basis of our results, and used in combination with CCR5 inhibitors, such as maraviroc (Selzentry), the only coreceptor-targeted drug in clinical use, pepRF1 could be a potent complement to improve the options available for patients predominantly infected with X4 or dual-tropic HIV-1 strains. Indeed, in more than 50% of HIV-1 infected individuals, CCR5-tropic viruses are usually present as mixtures together with CXCR4-using viruses.[56,57] A combination of CCR5 and CXCR4 inhibitors would also eliminate the current need to verify the tropism of the virus population, a factor that limits the use of maraviroc. Moreover, some reports have shown that HIV gp120 can trigger signaling and chemotactic events specifically through CCR5 and CXCR4, and in a CD4-independent manner.[58,59] Such effects induced by the viral envelope, could also be effectively blocked by CCR5/CXCR4 antagonists, showing an additional advantage of pepRF1.

Despite the growing interest in CXCR4 as a druggable target, the development of CXCR4 inhibitors has been challenging. In fact, to date no CXCR4 inhibitor has been approved for clinical use as an anti-HIV-1 agent. AMD3100 (Plerixafor, Mozobil), one of the most potent CXCR4 antagonist described, was initially developed to be used as an anti-HIV-1 drug[37,39] but clinical trials were interrupted due to undesired effects.[60,61] This molecule is now being used to mobilize hematopoietic stem cells from the bone marrow to the bloodstream.[60−63] Thus, the quest for druggable CXCR4-targeting compounds for the treatment of HIV-1 infection continues.

Like AMD3100, the selective antiviral activity of pepRF1 against CXCR4-tropic HIV strains is based on the specific inhibition of CXCR4-mediated virus entry via direct interaction with CXCR4, counteracting the effects of CXCL12, without triggering any response by itself upon binding to CXCR4.[37−39,47−49] In addition, the fact that pepRF1 is resistant to proteolytic degradation is also indicative of its potential use at low doses by oral administration.

CONCLUDING REMARKS−BEYOND HIV

Taken together, our findings point toward a promising role of pepRF1 as an anti-HIV-1 lead that could be used in the future, alone or in combination with other entry inhibitors, in order to block infection of CXCR4- and dual tropic (CXCR4 and CCR5)-HIV strains, and achieve measurable declines in overall plasma viremia delaying the progression of the disease. It is also worth stressing that pepRF1 could also be used as a novel therapeutic strategy for CXCR4-related diseases. CXCR4 is a G-protein-coupled receptor (GPCR) that, upon interaction with its cognate ligand chemokine CXCL12, activates a complex cascade of intracellular signaling pathways that regulate a large number of physiological processes including HIV-1 infectivity,[38,39,47,48] tumorigenesis,[64−70] stem cell migration,[71] autoimmune diseases,[72] and inflammation.[70] CXCR4 expression has been implicated in a variety of other diseases, such as rheumatoid arthritis,[73,74] atherosclerosis,[75] neurodegenerative diseases,[76] and various types of cancers where it plays a pivotal role in tumor development and metastasis.[64−70] This has been demonstrated for breast,[69] prostate,[77] lung,[65,78] and colorectal cancer,[79] as well as primary brain tumors such as glioblastoma.[80] Hence, the disruption of the CXCR4-CXCL12 axis by using a CXCR4-antagonist provides a promising molecular target for future specific therapies in areas beyond HIV-1 infection.

METHODS

pepR and pepR Derivative Synthesis. Peptides were synthesized in C-terminal carboxamide form on a Liberty Blue automated microwave peptide synthesizer (CEM Corporation, Matthews, NC) using Fmoc protocols. They were assembled at 0.05 mmol scale on a H-Rink Amide-ChemMatrix resin of 0.50 mmol/g substitution (PCAS BioMatrix, Montreal, Canada). Couplings were performed at 90 °C with 5-fold excess of Fmoc-amino acid/*N*,*N*′-diisopropylcarbodiimide (DIC)/Oxyma (1:2.5:5 molar ratio) in *N*,*N*-dimethylformamide (DMF), and deprotection with piperidine (20% v/v in DMF), followed by extensive DMF washes. After chain assembly, peptides were fully deprotected and cleaved from the resin by acidolysis with trifluoroacetic acid (TFA)/H_2O/3,6-dioxa-1,8-octanedithiol (DODT)/triisopropylsilane (TIS)

https://dx.doi.org/10.1021/acsinfecdis.9b00507
ACS Infect. Dis. 2021, 7, 6−22

(94:2.5:2.5:1 v/v) for 90 min. Peptides were precipitated by cold diethyl ether followed by 3 × 5 min centrifugation at 4800 rpm, 4 °C; the pellet was taken up in water and lyophilized. Crude peptides were inspected by analytical reversed-phase high-performance liquid chromatography (RP-HPLC) and liquid chromatography−mass spectrometry (LC-MS), and purified by preparative RP-HPLC (Figure S11) as described below. Fractions with the expected mass and with HPLC purity >95% were pooled and lyophilized.

RP-HPLC and LC-MS Analysis of pepR and Derivatives. Analytical RP-HPLC was performed on a LC-20AD instrument (Shimadzu, Kyoto, Japan) equipped with a Luna C18 column (4.6 mm × 50 mm, 3 μm; Phenomenex, Torrance, CA) using linear gradients of solvent B (0.036% v/v TFA in acetonitrile (ACN)) into A (0.045% v/v TFA in H_2O) over 15 min, with 1 mL/min flow rate and UV detection at 220 nm. Preparative RP-HPLC separations were performed on a LC-8A instrument (Shimadzu) fitted with a Luna C18 column (21.2 mm × 250 mm, 10 μm; Phenomenex), using linear gradients of solvent D (0.1% v/v TFA in ACN) into C (0.1% v/v TFA in H_2O) over 30 min, at a 25 mL/min flow rate. Mass spectrometry analysis was performed on an LC-MS 2010EV instrument (Shimadzu) fitted with an XBridge C18 column (4.6 mm × 150 mm, 3.5 μm, Waters, Cerdanyola del Vallès, Spain), eluting with linear gradients of F (0.08% v/v formic acid in ACN) into E (0.1% v/v formic acid in H_2O) over 15 min at a 1 mL/min flow rate.

pepR Stability Assay. To evaluate pepR stability *in vitro*, 100 μL aliquots containing 25% (v/v) prewarmed human serum (Sigma) and 250 μM pepR were incubated at 37 °C with gentle agitation. At different time points (0, 1, 5, 10, 20, 30, 60, and 90 min), the incubation was stopped by 20 μL trichloroacetic acid (15% v/v in H_2O). Samples were cooled in ice for 15 min, centrifuged at 13000 rpm for 10 min and the supernatant was collected and analyzed by analytical RP-HPLC and LC-MS as described above. Peak area was estimated by integration of chromatograms and percentage of remaining peptide at each time point was calculated relative to that at t_0. Kinetic data were fitted to an exponential decay model to determine the half-life ($t_{1/2}$).

Synthesis of the Peptide Conjugate pepRF1-NODA-GA. The peptide conjugate pepRF1-NODA-GA was prepared on resin by coupling of 4-(4,7-bis(2-(tert-butoxy)-2-oxoethyl)-1,4,7-triazacyclononan-1-yl)-5-(tert-butoxy)-5-oxopentanoic acid (NODA-GA(tBu)$_3$) to the N-terminus of a fully side chain-protected pepRF1 sequence. Briefly, the chelating agent NODA-GA(tBu)$_3$ (2.0 equiv per amine on resin) was preincubated for 30 min with 2-(1*H*-benzotriazol-1-yl)-1,1,3,3-tetramethyluronium hexafluorophosphate (HBTU; 2.0 equiv per carboxylate group). This solution was added to the peptidyl resin (ca. 50 mg) previously suspended in dimethylformamide (DMF) and *N*,*N*-diisopropylethylamine (DIPEA; 10.0 equiv per amine group). After stirring for 2 h at room temperature, the solution was removed by filtration and the resin was washed with DMF (3×) and CH_2Cl_2 (3×). Removal of the side chain-protecting groups as well as cleavage from the resin was performed with 95% TFA, 2.5% TIS, 2.5% H_2O for 2 h at room temperature. The cleavage solution was collected by filtration, concentrated, and the peptide conjugate precipitated with ice-cold diethyl ether, washed several times with the same solvent and dried under a nitrogen flow before lyophilization. The lyophilized product was dissolved in 0.1% (v/v) TFA in water and purified by semi preparative RP-HPLC (Gradient A) to yield the desired conjugate, characterized by ESI-MS and lyophilized. Purity by analytical RP-HPLC (Gradient A, 220 nm): >98%; retention time = 13.5 min. ESI−MS (+): calcd m/z for $[M]^+$ 2367.4, found 1184.5 $[M + 2H]^{2+}$, 790.1 $[M + 3H]^{3+}$, 592.8 $[M + 3H]^{3+}$.

Radiolabeling of pepRF1-NODA-GA with $^{67}Ga^{3+}$. $^{67}GaCl_3$ was prepared from ^{67}Ga-citrate (Mallinckrodt Medical, Netherlands) following a described procedure.[81] The pH of a $^{67}GaCl_3$ fraction (500 μL) eluted from the SEP-PAK cartridge was adjusted to pH 5 by adding 0.4 M sodium acetate solution (750 μL). Part of this solution (207 μL, 55.5 MBq) was added to the peptide conjugate (23 μL, 0.5 mM) and the mixture was incubated for 30 min at room temperature. The radiochemical purity (>95%) of the radiopeptide pepRF1^{67}Ga-NODA-GA was checked by RP-HPLC (Gradient B); retention time = 13.9 min.

pepRF1-NODA-GA and pepRF1-(^{67}Ga-NODA-GA). Analytical RP-HPLC of the peptide conjugate and radiolabeled peptide was performed on a PerkinElmer LC pump 200 equipment coupled to a Shimadzu SPD 10AV UV/vis detector and to a Berthold-LB 509 radiometric detector. Purification of pepRF1-NODA-GAwas accomplished by preparative RP-HPLC on a Waters 2535, quaternary gradient module, with a Waters 2998 photodiode array detector. Analytical control and semipreparative purifications were performed on Supelco Discovery Bio Wide Pore C18 Column (250 mm × 4.6 mm, 5 μm) and Supelco Discovery Bio Wide Pore C18 (250 mm × 10 mm, 10 μm) columns with a flow rate of 1.0 mL/min (analytical) or 2.0 mL/min (semipreparative), respectively. UV detection: λ = 220 nm; Eluents: (A) 0.1% TFA in H_2O; (B) 0.1% TFA in CH_3CN.

Applied binary HPLC gradients: Gradient A (analytical and semipreparative of peptide conjugate): 0−25 min, 10−50% B; 25−27 min, 100% B; 27−28 min, 100−0% B; 28−30 min, 10% B. Gradient B (^{67}Ga-labeled peptide conjugate): 0.0−25.0 min, 5%−100% B; 25−29.0 min, 100% B; 29.0−30.0 min; 100−5%.

Cell Culture. Human embryonic kidney 293T (HEK293T) and HeLa-derived TZM-bl cell lines, were purchased from the American Tissue Cell Culture Collection (ATCC) (Manassas, VA, USA). Cells were cultured in complete medium composed of Dulbecco's modified Eagle's medium (DMEM) supplemented with 10% (v/v) heat-inactivated fetal bovine serum (FBS) and 100 U/mL penicillin/streptomycin (Pen-Strep). THP-1 cells were obtained through the NIH AIDS Research and Reference Reagent Program, Division of AIDS, NIAID, NIH (Bethesda, MD, USA).[82] Cells were cultured in complete medium composed of Roswell Park Memorial Institute medium (RPMI-1640) supplemented with 10% (v/v) FBS and 100 U/mL Pen-Strep. MT4R5 cells[83] were grown in complete RPMI-1640 medium supplemented with 10% (v/v) heat-inactivated FBS and 100 U/mL Pen-Strep.

Flow cytometry assays were performed using primary CD4$^+$ T-lymphocytes isolated from PBMCs of a donor. Cell viability studies were performed using cryopreserved primary human CD4$^+$ T-lymphocytes and PBMCs purchased from Lonza (Basel, Switzerland). Primary CD4$^+$ T-lymphocytes and PBMCs were activated with 1 μg/mL of phytohemagglutinin (PHA) and were grown in complete RPMI-1640 medium supplemented with 10% (v/v) heat-inactivated FBS, 100 U/mL Pen-Strep, and IL-2 (100 IU/mL).

DMEM, RPMI-1640, FBS, and Pen-Strep were purchased from Gibco (Thermo-Fisher, Waltham, MA, USA). All cell

https://dx.doi.org/10.1021/acsinfecdis.9b00507
ACS Infect. Dis. 2021, 7, 6−22

cultures were maintained at 37 °C in a humidified atmosphere with 5% CO_2.

Virus Production. The full-length molecular clone pNL4.3, the env-defective molecular clone pNL4.3Δenv,[84] and the pHEF-VSVG[85] vector were obtained through the NIH AIDS Research and Reference Reagent Program, Division of AIDS, NIAID, NIH. Infectious HIV-$1_{NL4.3}$ viruses and env-defective HIV-$1_{NL4.3}$ viruses pseudotyped with VSVG (HIV-$1_{NL4.3}$-VSV-G) were produced by transfecting HEK293T cells with pNL4.3 and pNL4.3Δenv clones, respectively, through the calcium phosphate coprecipitation method.[86,87] Briefly, a total of 3.5 μg/well of plasmid DNA was used to transfect HEK293T cells (5×10^5 cells/well) in tissue culture-treated 6-well microplates from TPP (Trasadingen, Switzerland). Calcium-phosphate-DNA transfection mixtures were prepared by diluting plasmid DNA in 1 mM Tris-HCl, 0.1 mM EDTA, 250 mM $CaCl_2$, pH 7.6. The DNA mixture was then added to an equal volume of 50 mM HEPES (Merck, Darmstadt, Germany), 280 mM NaCl (Merck), 1.5 mM Na_2HPO_4(Merck), pH 7.05, under gentle agitation. Transfection mixtures were allowed to incubate at room temperature, for 20 min, before addition to cells. After 18 h, transfection mixtures were replaced with fresh complete medium. Viral supernatants were collected 48 h post-transfection, centrifuged at 315*g* for 5 min to remove cell debris, and stored at −80 °C until used.

Viral supernatants were titered by the Reed-Muench method[88] in a single-cycle viral infectivity assay on TZM-bl cells. TZM-bl cells contain a HIV long terminal repeat (LTR)-driven β-galactosidase and luciferase reporter cassettes that are activated by HIV-1 Tat expression. Briefly, TZM-bl cells were seeded at 2×10^4 cells/well in tissue culture-treated 96-well flat-bottomed polystyrene microplates (Corning, NY, USA), and incubated for 24 h. Cells were then incubated with 2-fold serial dilutions of viral supernatants for 3 h, after which the supernatant was replaced with fresh complete medium. After 45 h, infection of TZM-bl cells was quantified through luciferase reporter-gene expression levels[89,90] using the Luc-Screen luciferase chemiluminescence detection system (Thermo-Fisher), according to manufacturer instructions. Luminescence intensity, *L*, was measured in an Infinite M200 microplate reader from Tecan (Männedorf, Switzerland). Cells were considered infected if the respective luminescence intensity was 5-fold higher than the intensity of control cells (in the absence of viruses). Titration was performed with at least four replicates to allow accurate estimation of HIV-$1_{NL4.3}$ and HIV-$1_{NL4.3}$-VSV-G 50% tissue culture infectious dose ($TCID_{50}$) of viral supernatants.

To measure the inhibition potency on patient-derived viruses, we used several previously described full-length HIV-1 molecular clones carrying envelope sequences with different coreceptor tropism isolated from two patients plasma (patients T5 and T28).[44] Isolates X4−1 and X4−2 (from patient T28) are CXCR4-tropic, while isolates R5−1, R5−2, and R5−3 (from patient T5) are CCR5-tropic. Isolates R5X4−1 and R5X4−2 (from patient T5) are dual-tropic. Viral particles were produced by transfecting subconfluent HEK293T cells in T75 with 20 μg of each plasmid. DNA was diluted in 588 μL of H_2O with 195 μL of $CaCl_2$, and added to an equal volume of HEPES (Sigma-Aldrich, France) under agitation. Transfection mixtures were incubated at room temperature for 30 min, before addition to cells. After 16 h, transfection mixtures were replaced with fresh complete medium. Viral supernatants were collected 40 h post-transfection, centrifuged at 600*g* for 5 min to remove cell debris, filtered with 0.45 μm filter and stored at −80 °C until used. Viral supernatants were titered in a viral infection assay on TZM-bl cells. Twenty-four h before infection, 1×10^4TZM-bl cells/well were seeded in tissue culture-treated 96-well flat-bottom microplates. Cells were then incubated with several dilutions of viral supernatants. After 48 h, infection of TZM-bl cells was quantified using a chemiluminescent β-galactosidase reporter-gene expression assay (Roche, France), according to manufacturer instructions. *L* was measured in a Varioskan Flash device (Thermo Fisher Scientific).

The efficiency of viral entry into target cells was evaluated by the β-lactamase-Vpr assay.[41] Virus stocks for this assay were produced by transfection of subconfluent HEK293T cells in T75 flasks by Jet Pei (Polyplus Inc. Illkrich, France) following the manufacturer instructions. Twelve μg of pNL4.3 or pNLAd8[91] or pNL4.3DIM[92] and 4 μg of a plasmid coding the Vpr gene fused to the β-lactamase gene (a kind gift from Michael D. Miller) were cotransfected. Medium was changed 16 h later, and the virus-containing supernatant was collected 40 h post-transfection, filtered with 0.45 μm filter and overlaid on a 20% (w/v) sucrose cushion in a Beckman SW32 tube, after which particles were pelleted by centrifugation (98 000*g*, 4 °C) for 90 min. Viral pellets were resuspended in RPMI medium to obtain a 10-fold concentration as compared with the initial culture supernatant, separated into several aliquots, and frozen at −80 °C.

Viral Inhibition Assays. The anti-HIV activity of the peptides was evaluated through single-cycle viral infectivity assays using TZM-bl reporter cells, as previously described.[90,93] TZM-bl cells were seeded at 2×10^4 cells/well in tissue culture-treated 96-well flat-bottomed polystyrene microplates (Corning) and incubated for 24 h at 37 °C with 5% CO_2. Cells were then incubated for 3 h with 100 $TCID_{50}$/well of HIV-$1_{NL4.3}$ or HIV-$1_{NL4.3}$-VSV-G in the presence of 2-fold serial dilutions of pepR, covering the 0.004−5 μM range, and 4-fold serial dilutions of pepRF1 and pepR-derivatives, covering the 0.000005−5 μM range.

For time-of-addition experiments, serial dilutions of pepR (0.004−5 μM) and pepRF1 (0.000005−5 μM) were instead added to cells at −1, 0, +1, +2, +3, or +4 h relatively to the moment of infection with HIV-$1_{NL4.3}$. After a 3 h incubation period, cells were washed with PBS and fresh complete medium was added. To compare the antiviral activity of pepRF1 with known HIV-1 inhibitors, cells were incubated with HIV-$1_{NL4.3}$ alone or in combination to 1 μM of pepRF1, dextran sulfate, AMD3100 (>97% purity), T20 (>99% purity), and AZT (>90% purity). Dextran sulfate and AMD3100 were purchased from Sigma-Aldrich (St. Louis, MO, USA); T20 and AZT were obtained through the NIH AIDS Reagent Program). After 1 h, cells were washed with PBS to remove all unbound viruses and synchronize the infection, as described elsewhere.[35] 1 μM of pepRF1, dextran sulfate, AMD3100, T20, and AZT were then added to cells at +1, +2, +3, +4 h, relatively to the moment of the virus addition to cells. The concentration used corresponds to at least 100-fold the IC_{50} of each inhibitor, as established in a TZM-bl single-cycle infectivity assay (data not shown). Untreated cells were used as a control. Infection of TZM-bl cells was quantified 45 h later through luciferase reporter-gene expression levels as described above. *L* measurements were performed in an Infinite M200 microplate reader, converted to the fraction of inhibited viruses, f_a, and analyzed

https://dx.doi.org/10.1021/acsinfecdis.9b00507
ACS Infect. Dis. 2021, 7, 6−22

through a nonlinear regression with the classical dose−response relationship (median-effects model based on mass action):[94]

$$f_a = 1 - \frac{L}{L_0} \quad (1)$$

$$f_a = \frac{1}{1 + \left(\frac{IC_{50}}{[I]}\right)^m} \quad (2)$$

where L_0 is the luminescence intensity in the absence of the inhibitor, IC_{50} is the concentration that inhibits 50% of viral infection, m is a slope parameter equivalent to the Hill slope, and [I] is the inhibitor concentration. At least three independent experiments were performed for each assay.

Susceptibility to pepR and pepRF1 of Viruses Carrying Patient-Derived Envelope Glycoproteins. Twenty-four hours before infection, 1×10^4 TZM-bl cells/well were seeded in tissue culture-treated 96-well flat-bottom microplates. TZM-bl cells were treated prior to infection with 4-fold serial dilutions of pepR and pepRF1, covering the 0.0012−1.25 μM range. Cells were then incubated with the supernatant of cells transfected with the molecular clones expressing patient-derived envelope glycoproteins (R5−1, R5−2, R5−3, X4−1, and X4−2) or the laboratory strains NL4.3 (CXCR4-tropic) or NLAd8 (CCR5-tropic). After 40 h, infection of TZM-bl cells was quantified through β-galactosidase reporter-gene assay (Roche), according to manufacturer's instructions. L was measured in a Varioskan Flash instrument (Thermo Fisher Scientific). Inhibition of dual-tropic viruses R5X4−1 and R5X4−2 was measured using a single concentration of MVC (5 nM), or of the indicated peptide (312 nM), or a combination of MVC and peptide (5 nM and 312 nM, respectively).

Cell Viability Studies. The cytotoxic effect of pepR and pepRF1 on TZM-bl cells, $CD4^+$ T-lymphocytes, and PBMCs was studied using a resazurin reduction fluorometric assay (alamarBlue cell viability reagent, Invitrogen, Thermo-Fisher). Resazurin, the active compound in alamarBlue, is a blue dye that can be reduced to a pink fluorescent intermediate, resorufin, as a result of cell metabolic activity.

TZM-bl cells (2×10^4 cells/well) were seeded in tissue culture-treated 96-well black flat-bottomed polystyrene plates (Corning) and incubated for 24 h at 37 °C with 5% CO_2. Cells were then incubated for 3 h with 4-fold serial dilutions of pepR and pepRF1 covering the 0.3−80 μM range. After incubation, cells were washed with PBS, alamarBlue was added at a final concentration of 10% (v/v) and incubated for 3 h. In a complementary assay performed at the same time, after washing the cells with PBS, fresh complete DMEM medium was added and after 45 h, alamarBlue (10% v/v) was added to cells and incubated for 3 h. $CD4^+$ T-lymphocytes (1×10^5 cells/well) and PBMCs (1×10^5 cells/well), activated with 1 μg/mL PHA and 50 IU/mL IL-2, were seeded in tissue culture-treated 96-well black flat-bottomed polystyrene plates and incubated for 45 h with increasing concentrations of pepR and pepRF1 covering the 0.3−80 μM range. After incubation, alamarBlue was added to the cells and at a final concentration of 10% (v/v) and incubated for 12 h. In all assays untreated cells were used as a control.

After the incubation of cells with alamarBlue, resorufin production was monitored by measuring the fluorescent emission intensity (excitation 560 nm, emission 590 nm) in an Infinite M200 microplate reader. The percentage of metabolic active cells was expressed as the percentage of resazurin reduction relative to the reduction measured for the untreated sample after correcting the data with background fluorescence emission intensity from resazurin in cell-free medium, according to the following expression:

$$\%\text{of metabolic active cells} = \frac{I - I_{\text{background}}}{I_{\text{control}} - I_{\text{background}}} \times 100\% \quad (3)$$

where I corresponds to the resorufin fluorescence emission intensity in the presence of peptide, I_{control} to the fluorescence emission intensity in the absence of peptides, and $I_{\text{background}}$ to the background fluorescence emission from the nonreduced alamarBlue reagent. At least three independent experiments were performed for each assay.

***In Vivo* Tolerability Study.** Analysis of the maximum tolerated dose (MTD) of pepRF1 in Institute of Cancer Research (ICR) mice was performed by Eurofins Pharmacology Discovery Services Taiwan, Ltd. Male and female ICR mice weighing 25 ± 5 g were provided by BioLasco Taiwan (under Charles River Laboratories License). Animals were acclimated for 3 days prior to use and were confirmed to be in good health. The animals were housed in animal cages (Allentown, USA) with a space allocation of 30 × 19 × 13 cm. All animals were maintained in a controlled temperature (20−24 °C) and humidity (30−70%) environment with 12-h light/dark cycles. Free access to standard lab diet [MFG (Oriental Yeast Co., Ltd., Japan)] and autoclaved tap water were granted. All aspects of the work including housing, experimentation, and animal disposal were performed in general accordance with the Guide for the Care and Use of Laboratory Animals[95] in an AAALAC (Association for Assessment and Accreditation of Laboratory Animal Care)-accredited laboratory animal facility following protocol regulations reviewed and approved by the IACUC (Institutional Animal Care and Use Committee) at Pharmacology Discovery Services Taiwan, Ltd.

Animals were divided in four groups of two male and two female ICR mice, each. pepRF1 was dissolved in 0.9% (m/v) NaCl (saline; Sin-Tong, Taiwan) at 0.6, 2, and 6 mg/mL. Each group of animals was injected intravenously with 0.6, 2, and 6 mg/mL of pepRF1 or saline, respectively. A dosing volume at 5 mL/kg was applied to each group. Animals received an initial dose of 3 mg/kg. If the animals survived for 24 h, the dose for the next cohort was increased. If one or more animals died, the dose for the next cohort was decreased. The dosing scheme was as follows: 3 mg/kg, if no death, 10 mg/kg, if no death, 30 mg/kg; 3 mg/kg if no death, 10 mg/kg, if death, 5 mg/kg; 3 mg/kg if death, 1 mg/kg, if death, 0.3 mg/kg; 3 mg/kg if death, 1 mg/kg, if no death, 1.7 mg/kg. The testing stopped when all animals survived at the upper bound, or when three dose levels had been tested, or when the upper or lower bound had been reached. At each dose level, animals were observed for the presence of acute toxic symptoms (mortality, convulsions, tremors, muscle relaxation, sedation, etc.) and autonomic effects (diarrhea, salivation, lacrimation, vasodilation, piloerection, etc.) during the first 15 min, and again at 30 min. Body weights were recorded predose and at 72 h after treatment using a 0−1000 g electronic scale (Tanita Corporation, Japan). The animals were observed and mortality noted daily after compound administration until 72 h. Gross necropsy was performed on all animals without tissue collection.

https://dx.doi.org/10.1021/acsinfecdis.9b00507
ACS Infect. Dis. 2021, 7, 6−22

Biodistribution Studies. All animal experiments were performed in compliance with national and European regulations for animal treatment. The biodistribution of the radiolabeled peptide conjugate pepRF1-(^{67}Ga-NODA-GA) was evaluated in groups of 3 female CD-1 mice (randomly bred, Charles River) weighting approximately 25−28 g each. Animals were injected intravenously with 100 μL (3.3−7.5 MBq/90−202 μCi) of the preparation via the tail vein. The animals were housed in a temperature- and humidity-controlled room with a 12 h light/12 h dark schedule and maintained on normal diet *ad libitum*. Mice were sacrificed by cervical dislocation at different time points (15 min, 1, 4, and 24 h) postinjection (p.i.). The injected radioactive dose and the radioactivity remaining in the animal after sacrifice were measured in a dose calibrator (Capintec). The difference between the radioactivity in the injected and sacrificed animal was assumed to be due to total excretion from whole animal body. Blood samples were taken by cardiac puncture at sacrifice. Tissue samples of the main organs were then dissected, weighted and counted in a gamma counter (Berthold). Biodistribution results were expressed as percentage of the injected activity per gram tissue (% I.A./g).

Viral Particle Integrity Studies. The effect of the peptides on the integrity of the viral particles was first evaluated using a Western blot-based assay. 100 $TCID_{50}$ of HIV-$1_{NL4.3}$ were incubated with 5 μM of pepR or pepRF1, for 1 h at 37 °C. Untreated HIV-$1_{NL4.3}$ virions (in the absence of peptides), which will remain intact and be able to cross a 20% (w/v) sucrose cushion, were used as positive control for viral integrity. HIV-$1_{NL4.3}$ virions treated with 0.5% (v/v) Triton X-100 for 1 h, were used as negative controls for viral integrity (positive controls for viral disruption). Samples were then centrifuged through a 20% (w/v) sucrose cushion for 2 h at 40 000 rpm and 4 °C. The viral pellet was resuspended and lysed directly in Laemmli buffer composed of sodium dodecyl sulfate (SDS, 4% w/v), 125 mM Tris−HCl (pH 6.8), 2-mercaptoethanol (10% v/v), glycerol (20% v/v), and bromophenol blue (0.02% w/v). Viral proteins were denatured by boiling for 10 min at 95 °C. Proteins were then separated by 12% (w/v) SDS-PAGE (National Diagnostics, Atlanta, GA, USA), transferred to nylon membranes (Hybond, Amersham Biosciences, GE Healthcare Life Sciences, Chicago, IL, USA), and reacted with anti-HIV p24 mAb (NIH AIDS Reagent Program, Division of AIDS, NIAID).[96,97] Membranes were then incubated with goat antimouse IgG (H+L)-HRP conjugate (Bio-Rad, Milan, Italy) and visualized by enhanced chemiluminescence (ECL) (Amersham Biosciences, GE Healthcare, BM, UK) using the Chemidoc XRS+ System (Bio-Rad, Hercules, CA, USA).

A complementary assay was also performed to investigate the integrity of viral particles using the QuickTiterLentivirus Titer Kit from Cell Biolabs (San Diego, CA, USA), which is an enzyme immunoassay developed for the specific detection and quantification of HIV-1 capsid (CA) protein (p24) associated with intact viral particles only. This can be achieved through the use of viral bind lentivirus reagents (ViraBind, patented technology) that form complexes with the intact virions while free p24 remain in the supernatant. Briefly, HIV-$1_{NL4.3}$ virions (100 $TCID_{50}$) were incubated with 5 μM of pepR or pepRF1 for 1 h at 37 °C. After incubation, a virus pulldown (using the ViraBind lentivirus reagents in the QuickTiterLentivirus Titer Kit) was performed to recover intact viral particles from viral supernatants. Virions were disrupted using sample diluent (QuickTiterLentivirus Titer Kit) and then added to an anti-p24 antibody-coated plate, and incubated for 4 h at 37 °C. Detection of viral-associated p24 protein was performed using FITC-conjugated anti-p24 mAb followed by HRP-conjugated anti-FITC mAb (QuickTiterLentivirus Titer Kit) following manufacturer instructions. Quantification of HIV-$1_{NL4.3}$p24 protein was determined by adding HRP-substrate solution to each sample followed by measuring absorbance at 450 nm. Untreated HIV-$1_{NL4.3}$ virions (in the absence of peptides) were used as positive control for viral integrity. HIV-$1_{NL4.3}$ virions treated with 70% (v/v) ethanol or 0.5% (v/v) Triton X-100 for 1 h, were used as negative controls for viral integrity (positive controls for viral disruption). At least three independent experiments were performed for each assay.

β-Lactamase Viral Fusion Assay. To measure the efficiency of virus entry into target cells, and the impact of peptides on this process, we used a previously described Vpr-BlaM assay.[41] In this assay, the β-lactamase enzyme fused to the viral protein Vpr is incorporated into virions and delivered into the cytosol of target cells, where β-lactamase activity can be quantified by the cleavage of a fluorescent substrate (CCF2). To this end, 2.0 × 10^5MT4R5 cells treated with a 4-fold serial dilution of pepR, pepRF1 and T20 covering the 0.0003−1.25 μM concentration range were exposed to the virus preparation of Blam NL4.3, Blam NLAD8 or Blam NL4.3-DIM for 4 h at 37 °C, using a virus concentration that leads to on approximately 30% of positive cells in the absence of treatment.

Cells were then washed and loaded with the CCF2 substrate (CCF2-AM loading kit, Invitrogen) in the presence of 1.8 mM probenecid (Sigma-Aldrich). Cells were incubated overnight at 15 °C with CO_2 independent medium (Invitrogen), washed with PBS containing 1% (w/v) BSA and 0.05% (w/v) saponin (Sigma-Aldrich) and fixed with paraformaldehyde (PFA). The cleaved CCF2 fluorescence emission intensity was measured by flow cytometry with excitation at 405 nm and emissions at 448 nm (cleaved CCF2-AM) and 525 nm (uncleaved CCF2-AM), on a FacsCanto II system with FACSDiva software (BD Bioscience). FlowJo, version 10 (Tree Star), was used to analyze and quantify the data.

Expression of HIV Coreceptors. The level of expression of CXCR4 on the cell surface was studied by flow cytometry using two different anti-CXCR4 mAbs, targeting two distinct epitopes: 12G5 (PE mouse antihuman CD184 clone 12G5 (RUO), BD Biosciences) and 1D9 (PE rat antihuman CD184 clone 1D9 (RUO), BD Biosciences). Activated primary $CD4^+$ T-lymphocytes were incubated for 90 min at 37 °C with a 4-fold serial dilution of pepR, pepRF1 and T20 covering the 0.0012−1.25 μM range, or a 4-fold serial dilution of the CXCR4-antagonist AMD3100 covering the 0.049−50 μM range, or a 4-fold serial dilution of CXCL12 covering the 0.098−100 nM range. Then, each sample was split into two aliquots and the cells were separately stained with the two mAbs in the presence of PBS-BSA 1% (w/v) 45 min at room temperature in the dark.

The expression of CCR5 on the cell surface was studied using human CCR5 fluorescein mAb (clone 45502) (R&D Systems). Activated primary $CD4^+$ T lymphocytes were incubated 10 min at room temperature with three dilutions (1250, 78, 5 nM) of pepR, pepRF1, T20 and AMD3100. Then, the cells were stained with the mAb in the presence of PBS-BSA 1% (w/v) 45 min at 4 °C in the dark. Fluorescence emission intensity was measured by flow cytometry on a

https://dx.doi.org/10.1021/acsinfecdis.9b00507
ACS Infect. Dis. 2021, 7, 6−22

FacsCanto II system with FACSDiva software (BD Bioscience). FlowJo, version 10 (Tree Star), was used to analyze and quantify the data.

Intracellular Ca^{2+} Mobilization Assay. CXCR4-mediated intracellular Ca^{2+} mobilization was assessed using a Fluo-4-based fluorescence assay.[98] Fluo-4 is a fluorescently labeled probe that exhibits an increase in fluorescence emission intensity upon binding to Ca^{2+}.[99] Fluo-4 AM ester (Invitrogen, Thermo-Fisher) was dissolved in pure DMSO (Merck) to a final concentration of 4 mM. Fluo-4 stock solutions were diluted to final working concentrations in Hank's Balanced Salt Solution (HBSS, Gibco, Thermo-Fisher). DMSO content was kept below 0.25% (v/v) to prevent cell death.

THP-1 monocytes were cultured in complete RPMI medium. Cells were washed with HBSS, resuspended in HBSS with 5 μM Fluo-4, at a density of 2.5×10^6 cells/mL, and incubated for 1 h at 37 °C, to allow Fluo-4 probe internalization into the cytosol. To remove the extracellular probe, cells were washed and resuspended in fresh HBSS and allowed to stabilize for 10 min at 37 °C, before starting fluorescence measurements.

Variations in cytosolic Ca^{2+} levels were followed by time-resolved Fluo-4 fluorescence emission intensity measurements. Measurements were carried out in a FLS920 spectrofluorometer (Edinburgh Instruments, Livingston, UK) at 37 °C. The excitation and emission wavelengths were 491 and 519 nm, respectively. Excitation and emission slits were 3 and 8 nm, respectively. Fluorescence emission intensity of labeled cells (1.25×10^6 cells/mL) was collected for 30 s, before addition of CXCL12 (Sigma, 50 nM), pepR (1.25 μM), pepRF1 (1.25 μM), or AMD3100 (50 μM), individually or in combination, after which the signal was collected for an additional 270 s. Data was corrected for dilution and background noise. CXCL12 and inhibitors solutions were prepared in HBSS. At least three independent experiments were performed for each assay.

Statistical Analysis. Statistical analysis was performed using GraphPad Prism version 7.0 for Macintosh (GraphPad Software, San Diego, California USA, www.graphpad.com). Data are presented as mean ± standard deviation of three independent experiments performed, unless indicated otherwise.

■ ASSOCIATED CONTENT

Supporting Information

The Supporting Information is available free of charge at https://pubs.acs.org/doi/10.1021/acsinfecdis.9b00507.

pepR stability in human serum (Figure S1), Mass spectra of pepR fragments (Figure S2), Cytotoxicity of pepR and pepRF1 (Figure S3), Evaluation of pepR time-of-action (Figure S4), Antiviral activity of pepR against HIV-1NL4.3-VSV-G (Figure S5), Effect of pepR and pepRF1 on the integrity of viral particles (Figure S6), pepR inhibits HIV-1 cell entry in a coreceptor specific manner and inhibits CXCR4-tropic HIV-1 clones carrying patient-derived envelope glycoprotein (Figure S7), CXCR4 recognition by pepR (Figure S8), CCR5 recognition by pepR and pepRF1 (Figure S9), Impact of pepR on CXCR4-associated Ca^{2+} intracellular mobilization (Figure S10), Analytical reverse-phase HPLC and ESI-MS of purified pepR and pepRF1 (Figure S11) (PDF)

■ AUTHOR INFORMATION

Corresponding Authors

Fabrizio Mammano − *INSERM UMR 1124, Université de Paris, F-75006 Paris, France;* orcid.org/0000-0002-9193-7696; Email: fabrizio.mammano@inserm.fr

David Andreu − *Department of Experimental and Health Sciences, Universitat Pompeu Fabra, 08003 Barcelona, Spain;* orcid.org/0000-0002-6317-6666; Email: david.andreu@upf.edu

Miguel A. R. B. Castanho − *Instituto de Medicina Molecular, Faculdade de Medicina, Universidade de Lisboa, 1649-028 Lisboa, Portugal;* orcid.org/0000-0001-7891-7562; Email: macastanho@medicina.ulisboa.pt

Ana Salomé Veiga − *Instituto de Medicina Molecular, Faculdade de Medicina, Universidade de Lisboa, 1649-028 Lisboa, Portugal;* orcid.org/0000-0002-9892-2243; Email: aveiga@medicina.ulisboa.pt

Authors

Iris Cadima-Couto − *Instituto de Medicina Molecular, Faculdade de Medicina, Universidade de Lisboa, 1649-028 Lisboa, Portugal*

Alexandra Tauzin − *INSERM UMR 1124, Université de Paris, F-75006 Paris, France*

João M. Freire − *Instituto de Medicina Molecular, Faculdade de Medicina, Universidade de Lisboa, 1649-028 Lisboa, Portugal*

Tiago N. Figueira − *Instituto de Medicina Molecular, Faculdade de Medicina, Universidade de Lisboa, 1649-028 Lisboa, Portugal;* orcid.org/0000-0002-0813-0745

Rúben D. M. Silva − *Centro de Ciências e Tecnologias Nucleares and Departamento de Engenharia e Ciências Nucleares, Instituto Superior Técnico, Universidade de Lisboa, 2695-066 Bobadela, LRS, Portugal*

Clara Pérez-Peinado − *Department of Experimental and Health Sciences, Universitat Pompeu Fabra, 08003 Barcelona, Spain*

Catarina Cunha-Santos − *Research Institute for Medicines (iMed.ULisboa), Faculdade de Farmácia, Universidade de Lisboa, 1649-003 Lisboa, Portugal;* orcid.org/0000-0001-8789-1966

Inês Bártolo − *Research Institute for Medicines (iMed.ULisboa), Faculdade de Farmácia, Universidade de Lisboa, 1649-003 Lisboa, Portugal*

Nuno Taveira − *Research Institute for Medicines (iMed.ULisboa), Faculdade de Farmácia, Universidade de Lisboa, 1649-003 Lisboa, Portugal; Centro de Investigação Interdisciplinar Egas Moniz (CiiEM), Instituto Universitário Egas Moniz, 2829-511 Monte de Caparica, Portugal*

Lurdes Gano − *Centro de Ciências e Tecnologias Nucleares and Departamento de Engenharia e Ciências Nucleares, Instituto Superior Técnico, Universidade de Lisboa, 2695-066 Bobadela, LRS, Portugal*

João D. G. Correia − *Centro de Ciências e Tecnologias Nucleares and Departamento de Engenharia e Ciências Nucleares, Instituto Superior Técnico, Universidade de Lisboa, 2695-066 Bobadela, LRS, Portugal;* orcid.org/0000-0002-7847-4906

Joao Goncalves − *Research Institute for Medicines (iMed.ULisboa), Faculdade de Farmácia, Universidade de Lisboa, 1649-003 Lisboa, Portugal*

Complete contact information is available at: https://pubs.acs.org/10.1021/acsinfecdis.9b00507

Notes

The authors declare no competing financial interest.

■ ACKNOWLEDGMENTS

This work was supported by Fundação para a Ciência e a Tecnologia (FCT-MCTES, Portugal) project PTDC/QEQ-MED/4412/2014, and by the Institut National de la Santé et de la Recherche Médicale (Inserm). I.C.C., J.M.F., T.N.F., and I.B. acknowledge fellowships SFRH/BPD/65531/2009, SFRH/BD/70423/2010, SFRH/BD/5283/2013, and SFRH/BPD/76225/2011, respectively, funded by FCT-MCTES. A.T. is the recipient of a fellowship from Agence Nationale de Recherche sur le Sida et les Hépatites Virales (ANRS). A.S.V. acknowledges funding under the Investigator Programme (IF/00803/2012) from FCT-MCTES. Work at Pompeu Fabra University was supported by grants AGL2014-52395-C2 and AGL2017-84097-C2-2-R and by the "María de Maeztu" Program for Units of Excellence in R&D from the Spanish Ministry of Innovation and Competitiveness (MINECO). The following reagents were obtained through the NIH AIDS Reagent Program, Division of AIDS, NIAID, NIH: pNL4.3 from Dr. Malcolm Martin (Cat# 114);[43] pNL(AD8) from Eric O. Freed (Cat# 11346);[91] pNL4.3Δenv from Dr. Haili Zhang, Dr. Yan Zhou, and Dr. Robert Siliciano (Cat# 11100);[84] pHEF-VSVG vector from Dr. Lung-Ji Chang (Cat# 4693);[85] T-20 (Enfuvirtide) (Cat# 12732); Zidovudine (AZT) (Cat# 3485); Anti-HIV-1 p24 Monoclonal (183-H12-5C) from Dr. Bruce Chesebro and Kathy Wehrly (Cat# 3537).[96,97] THP-1 NCI Cells from Drs. Li Wu and Vineet N. Kewal Ramani (Cat# 9940).[82]

■ REFERENCES

(1) Moir, S., Chun, T.-W., and Fauci, A. S. (2011) Pathogenic Mechanisms of HIV Disease. *Annu. Rev. Pathol.: Mech. Dis. 6* (1), 223−248.

(2) UNAIDS, Global HIV & AIDS Statistics − 2020 Fact Sheet. https://www.unaids.org/en/resources/fact-sheet (accessed Oct 03, 2020).

(3) Gunthard, H. F., Aberg, J. A., Eron, J. J., Hoy, J. F., Telenti, A., Benson, C. A., Burger, D. M., Cahn, P., Gallant, J. E., Glesby, M. J., Reiss, P., Saag, M. S., Thomas, D. L., Jacobsen, D. M., and Volberding, P. A. (2014) International Antiviral Society-USA Panel. Antiretroviral Treatment of Adult HIV Infection: 2014 Recommendations of the International Antiviral Society-USA Panel. *JAMA 312* (4), 410−425.

(4) Vlieghe, P., Lisowski, V., Martinez, J., and Khrestchatisky, M. (2010) Synthetic Therapeutic Peptides: Science and Market. *Drug Discovery Today 15* (1−2), 40−56.

(5) Kaspar, A. A., and Reichert, J. M. (2013) Future Directions for Peptide Therapeutics Development. *Drug Discovery Today 18* (17−18), 807−817.

(6) Castel, G., Chtéoui, M., Heyd, B., and Tordo, N. (2011) Phage Display of Combinatorial Peptide Libraries: Application to Antiviral Research. *Molecules 16* (5), 3499−3518.

(7) Rausch, D. M., Hwang, K. M., Padgett, M., Voltz, A. H., Rivas, A., Engleman, E., Gaston, I., McGrath, M., Fraser, B., Kalyanaraman, V. S., et al. (1990) Peptides Derived from the CDR3-Homologous Domain of the CD4Molecule Are Specific Inhibitors of HIV-1 and SIV Infection, Virus-Induced Cell Fusion, and Postinfection Viral Transmission in Vitro. Implications for the Design of Small Peptide Anti-HIV Therap. *Ann. N. Y. Acad. Sci. 616*, 125−128.

(8) Jin, B. S., Ryu, J. R., Ahn, K., and Yu, Y. G. (2000) Design of a Peptide Inhibitor That Blocks the Cell Fusion Mediated by Glycoprotein 41 of Human Immunodeficiency Virus Type 1. *AIDS Res. Hum. Retroviruses 16* (17), 1797−1804.

(9) Gleenberg, I. O., Herschhorn, A., and Hizi, A. (2007) Inhibition of the Activities of Reverse Transcriptase and Integrase of Human Immunodeficiency Virus Type-1 by Peptides Derived from the Homologous Viral Protein R (Vpr). *J. Mol. Biol. 369* (5), 1230−1243.

(10) Agopian, A., Gros, E., Aldrian-Herrada, G., Bosquet, N., Clayette, P., and Divita, G. (2009) A New Generation of Peptide-Based Inhibitors Targeting HIV-1 Reverse Transcriptase Conformational Flexibility. *J. Biol. Chem. 284* (1), 254−264.

(11) Gleenberg, I. O., Avidan, O., Goldgur, Y., Herschhorn, A., and Hizi, A. (2005) Peptides Derived from the Reverse Transcriptase of Human Immunodeficiency Virus Type 1 as Novel Inhibitors of the Viral Integrase. *J. Biol. Chem. 280* (23), 21987−21996.

(12) Li, H. Y., Zawahir, Z., Song, L. D., Long, Y. Q., and Neamati, N. (2006) Sequence-Based Design and Discovery of Peptide Inhibitors of HIV-1 Integrase: Insight into the Binding Mode of the Enzyme. *J. Med. Chem. 49* (15), 4477−4486.

(13) Schramm, H. J., Boetzel, J., Buttner, J., Fritsche, E., Gohring, W., Jaeger, E., Konig, S., Thumfart, O., Wenger, T., and Nagel, N. E. (1996) The Inhibition of Human Immunodeficiency Virus Proteases by "Interface Peptides. *Antiviral Res. 30* (2−3), 155−170.

(14) Louis, J. M., Dyda, F., Nashed, N. T., Kimmel, A. R., and Davies, D. R. (1998) Hydrophilic Peptides Derived from the Transframe Region of Gag-Pol Inhibit the HIV-1 Protease. *Biochemistry 37* (8), 2105−2110.

(15) Kilby, J. M., Hopkins, S., Venetta, T. M., DiMassimo, B., Cloud, G. A., Lee, J. Y., Alldredge, L., Hunter, E., Lambert, D., Bolognesi, D., Matthews, T., Johnson, M. R., Nowak, M. A., Shaw, G. M., and Saag, M. S. (1998) Potent Suppression of HIV-1 Replication in Humans by T-20, a Peptide Inhibitor of Gp41-Mediated Virus Entry. *Nat. Med. 4* (11), 1302−1307.

(16) Lalezari, J. P., Henry, K., O'Hearn, M., Montaner, J. S. G., Piliero, P. J., Trottier, B., Walmsley, S., Cohen, C., Kuritzkes, D. R., Eron, J. J., Jr., Chung, J., DeMasi, R., Donatacci, L., Drobnes, C., Delehanty, J., and Salgo, M. (2003) TORO 1 Study Group. Enfuvirtide, an HIV-1 Fusion Inhibitor, for Drug-Resistant HIV Infection in North and South America. *N. Engl. J. Med. 348* (22), 2175−2185.

(17) Lazzarin, A., Clotet, B., Cooper, D., Reynes, J., Arasteh, K., Nelson, M., Katlama, C., Stellbrink, H.-J., Delfraissy, J.-F., Lange, J., Huson, L., DeMasi, R., Wat, C., Delehanty, J., Drobnes, C., and Salgo, M. (2003) TORO 2 Study Group. Efficacy of Enfuvirtide in Patients Infected with Drug-Resistant HIV-1 in Europe and Australia. *N. Engl. J. Med. 348* (22), 2186−2195.

(18) Doms, R. W., and Trono, D. (2000) The Plasma Membrane as a Combat Zone in the HIV Battlefield. *Genes Dev. 14* (21), 2677−2688.

(19) Rimsky, L. T., Shugars, D. C., and Matthews, T. J. (1998) Determinants of Human Immunodeficiency Virus Type 1 Resistance to Gp41-Derived Inhibitory Peptides. *J. Virol. 72* (2), 986−993.

(20) Golding, H., Zaitseva, M., de Rosny, E., King, L. R., Manischewitz, J., Sidorov, I., Gorny, M. K., Zolla-Pazner, S., Dimitrov, D. S., and Weiss, C. D. (2002) Dissection of Human Immunodeficiency Virus Type 1 Entry with Neutralizing Antibodies to Gp41 Fusion Intermediates. *J. Virol. 76* (13), 6780−6790.

(21) Welch, B. D., Francis, J. N., Redman, J. S., Paul, S., Weinstock, M. T., Reeves, J. D., Lie, Y. S., Whitby, F. G., Eckert, D. M., Hill, C. P., Root, M. J., and Kay, M. S. (2010) Design of a Potent D-Peptide HIV-1 Entry Inhibitor with a Strong Barrier to Resistance. *J. Virol. 84* (21), 11235−11244.

(22) Wei, X., Decker, J. M., Liu, H., Zhang, Z., Arani, R. B., Kilby, J. M., Saag, M. S., Wu, X., Shaw, G. M., and Kappes, J. C. (2002) Emergence of Resistant Human Immunodeficiency Virus Type 1 in Patients Receiving Fusion Inhibitor (T-20) Monotherapy. *Antimicrob. Agents Chemother. 46* (6), 1896−1905.

(23) Matthews, T., Salgo, M., Greenberg, M., Chung, J., DeMasi, R., and Bolognesi, D. (2004) Enfuvirtide: The First Therapy to Inhibit the Entry of HIV-1 into Host CD4 Lymphocytes. *Nat. Rev. Drug Discovery 3* (3), 215−225.

(24) Naider, F., and Anglister, J. (2009) Peptides in the Treatment of AIDS. *Curr. Opin. Struct. Biol. 19* (4), 473−482.

(25) Ashkenazi, A., Wexler-Cohen, Y., and Shai, Y. (2011) Multifaceted Action of Fuzeon as Virus-Cell Membrane Fusion Inhibitor. *Biochim. Biophys. Acta, Biomembr. 1808* (10), 2352−2358.
(26) Wang, G. (2012) Natural Antimicrobial Peptides as Promising Anti-HIV Candidates. *Curr. Top. Pept. Protein Res. 13*, 93−110.
(27) Qureshi, A., Thakur, N., and Kumar, M. (2013) HIPdb: A Database of Experimentally Validated HIV Inhibiting Peptides. *PLoS One 8* (1), e54908.
(28) Freire, J. M., Veiga, A. S., Conceição, T. M., Kowalczyk, W., Mohana-Borges, R., Andreu, D., Santos, N. C., Da Poian, A. T., and Castanho, M. A. R. B. (2013) Intracellular Nucleic Acid Delivery by the Supercharged Dengue Virus Capsid Protein. *PLoS One 8* (12), e81450.
(29) Freire, J. M., Veiga, A. S., Rego de Figueiredo, I., de la Torre, B. G., Santos, N. C., Andreu, D., Da Poian, A. T., and Castanho, M. A. R. B. (2014) Nucleic Acid Delivery by Cell Penetrating Peptides Derived from Dengue Virus Capsid Protein: Design and Mechanism of Action. *FEBS J. 281* (1), 191−215.
(30) Freire, J. M., Almeida Dias, S., Flores, L., Veiga, A. S., and Castanho, M. A. R. B. (2015) Mining Viral Proteins for Antimicrobial and Cell-Penetrating Drug Delivery Peptides. *Bioinformatics 31* (14), 2252−2256.
(31) Bottger, R., Hoffmann, R., and Knappe, D. (2017) Differential Stability of Therapeutic Peptides with Different Proteolytic Cleavage Sites in Blood, Plasma and Serum. *PLoS One 12* (6), No. e0178943.
(32) Bergmann, R., Scheunemann, M., Heichert, C., Mäding, P., Wittrisch, H., Kretzschmar, M., Rodig, H., Tourwé, D., Iterbeke, K., Chavatte, K., Zips, D., Reubi, J. C., and Johannsen, B. (2002) Biodistribution and Catabolism of (18)F-Labeled Neurotensin(8−13) Analogs. *Nucl. Med. Biol. 29* (1), 61−72.
(33) Neves, V., Aires-Da-Silva, F., Morais, M., Gano, L., Ribeiro, E., Pinto, A., Aguiar, S., Gaspar, D., Fernandes, C., Correia, J. D. G., and Castanho, M. A.R.B. (2017) Novel Peptides Derived from Dengue Virus Capsid Protein Translocate Reversibly the Blood-Brain Barrier through a Receptor-Free Mechanism. *ACS Chem. Biol. 12* (5), 1257−1268.
(34) Frankel, A. D., and Young, J. A. T. (1998) HIV-1: Fifteen Proteins and an RNA. *Annu. Rev. Biochem. 67* (1), 1−25.
(35) Daelemans, D., Pauwels, R., De Clercq, E., and Pannecouque, C. (2011) A Time-of-Drug Addition Approach to Target Identification of Antiviral Compounds. *Nat. Protoc. 6* (6), 925−933.
(36) Ito, M., Baba, M., Sato, A., Pauwels, R., De Clercq, E., and Shigeta, S. (1987) Inhibitory Effect of Dextran Sulfate and Heparin on the Replication of Human Immunodeficiency Virus (HIV) in Vitro. *Antiviral Res. 7* (6), 361−367.
(37) De Clercq, E., Yamamoto, N., Pauwels, R., Balzarini, J., Witvrouw, M., De Vreese, K., Debyser, Z., Rosenwirth, B., Peichl, P., and Datema, R. (1994) Highly Potent and Selective Inhibition of Human Immunodeficiency Virus by the Bicyclam Derivative JM3100. *Antimicrob. Agents Chemother. 38* (4), 668−674.
(38) Schols, D., Struyf, S., Van Damme, J., Este, J. A., Henson, G., and De Clercq, E. (1997) Inhibition of T-Tropic HIV Strains by Selective Antagonization of the Chemokine Receptor CXCR4. *J. Exp. Med. 186* (8), 1383−1388.
(39) Donzella, G. A., Schols, D., Lin, S. W., Este, J. A., Nagashima, K. A., Maddon, P. J., Allaway, G. P., Sakmar, T. P., Henson, G., De Clercq, E., and Moore, J. P. (1998) AMD3100, a Small Molecule Inhibitor of HIV-1 Entry via the CXCR4 Co-Receptor. *Nat. Med. 4* (1), 72−77.
(40) Gonzalez-Ortega, E., Mena, M.-P., Permanyer, M., Ballana, E., Clotet, B., and Este, J. A. (2010) ADS-J1 Inhibits HIV-1 Entry by Interacting with Gp120 and Does Not Block Fusion-Active Gp41 Core Formation. *Antimicrob. Agents Chemother. 54* (10), 4487−4492.
(41) Cavrois, M., De Noronha, C., and Greene, W. C. (2002) A Sensitive and Specific Enzyme-Based Assay Detecting HIV-1 Virion Fusion in Primary T Lymphocytes. *Nat. Biotechnol. 20* (11), 1151−1154.
(42) Daecke, J., Fackler, O. T., Dittmar, M. T., and Krausslich, H.-G. (2005) Involvement of Clathrin-Mediated Endocytosis in Human Immunodeficiency Virus Type 1 Entry. *J. Virol. 79* (3), 1581−1594.
(43) Adachi, A., Gendelman, H. E., Koenig, S., Folks, T., Willey, R., Rabson, A., and Martin, M. A. (1986) Production of Acquired Immunodeficiency Syndrome-Associated Retrovirus in Human and Nonhuman Cells Transfected with an Infectious Molecular Clone. *J. Virol. 59* (2), 284−291.
(44) Skrabal, K., Saragosti, S., Labernardiere, J.-L., Barin, F., Clavel, F., and Mammano, F. (2005) Human Immunodeficiency Virus Type 1 Variants Isolated from Single Plasma Samples Display a Wide Spectrum of Neutralization Sensitivity. *J. Virol. 79* (18), 11848−11857.
(45) Berger, E. A., Doms, R. W., Fenyö, E.-M., Korber, B. T. M., Littman, D. R., Moore, J. P., Sattentau, Q. J., Schuitemaker, H., Sodroski, J., and Weiss, R. A. (1998) A New Classification for HIV-1. *Nature 391* (6664), 240.
(46) Dorr, P., Westby, M., Dobbs, S., Griffin, P., Irvine, B., Macartney, M., Mori, J., Rickett, G., Smith-Burchnell, C., Napier, C., Webster, R., Armour, D., Price, D., Stammen, B., Wood, A., and Perros, M. (2005) Maraviroc (UK-427,857), a Potent, Orally Bioavailable, and Selective Small-Molecule Inhibitor of Chemokine Receptor CCR5 with Broad-Spectrum Anti-Human Immunodeficiency Virus Type 1 Activity. *Antimicrob. Agents Chemother. 49* (11), 4721−4732.
(47) Oberlin, E., Amara, A., Bachelerie, F., Bessia, C., Virelizier, J. L., Arenzana-Seisdedos, F., Schwartz, O., Heard, J. M., Clark-Lewis, I., Legler, D. F., Loetscher, M., Baggiolini, M., and Moser, B. (1996) The CXC Chemokine SDF-1 Is the Ligand for LESTR/Fusin and Prevents Infection by T-Cell-Line-Adapted HIV-1. *Nature 382* (6594), 833−835.
(48) Mishra, R. K., Shum, A. K., Platanias, L. C., Miller, R. J., and Schiltz, G. E. (2016) Discovery and Characterization of Novel Small-Molecule CXCR4 Receptor Agonists and Antagonists. *Sci. Rep. 6*, 1−9.
(49) Zirafi, O., Kim, K.-A., Standker, L., Mohr, K. B., Sauter, D., Heigele, A., Kluge, S. F., Wiercinska, E., Chudziak, D., Richter, R., Moepps, B., Gierschik, P., Vas, V., Geiger, H., Lamla, M., Weil, T., Burster, T., Zgraja, A., Daubeuf, F., Frossard, N., Hachet-Haas, M., Heunisch, F., Reichetzeder, C., Galzi, J., Pérez-Castells, J., Canales-Mayordomo, A., Jiménez-Barbero, J., Giménez-Gallego, G., Schneider, M., Shorter, J., Telenti, A., Hocher, B., Forssmann, W., Bonig, H., Kirchhoff, F., and Münch, J. (2015) Discovery and Characterization of an Endogenous CXCR4 Antagonist. *Cell Rep. 11* (5), 737−747.
(50) Carnec, X., Quan, L., Olson, W. C., Hazan, U., and Dragic, T. (2005) Anti-CXCR4Monoclonal Antibodies Recognizing Overlapping Epitopes Differ Significantly in Their Ability to Inhibit Entry of Human Immunodeficiency Virus Type 1. *J. Virol. 79* (3), 1930−1933.
(51) Hatse, S., Princen, K., Bridger, G., De Clercq, E., and Schols, D. (2002) Chemokine Receptor Inhibition by AMD3100 Is Strictly Confined to CXCR4. *FEBS Lett. 527* (1−3), 255−262.
(52) Choi, W.-T., and An, J. (2011) Biology and Clinical Relevance of Chemokines and Chemokine Receptors CXCR4 and CCR5 in Human Diseases. *Exp. Biol. Med. 236* (6), 637−647.
(53) Adlere, I., Caspar, B., Arimont, M., Dekkers, S., Visser, K., Stuijt, J., de Graaf, C., Stocks, M., Kellam, B., Briddon, S., Wijtmans, M., de Esch, I., Hill, S., and Leurs, R. (2019) Modulators of CXCR4 and CXCR7/ACKR3 Function. *Mol. Pharmacol. 96* (6), 737−752.
(54) Connor, R. I., Sheridan, K. E., Ceradini, D., Choe, S., and Landau, N. R. (1997) Change in Coreceptor Use Correlates with Disease Progression in HIV-1–Infected Individuals. *J. Exp. Med. 185* (4), 621−628.
(55) Wagner, T. A., and Frenkel, L. M. (2008) Potential Limitation of CCR5 Antagonists: Drug Resistance More Often Linked to CXCR4-Utilizing than to CCR5-Utilizing HIV-1. *AIDS 22* (17), 2393−2395.
(56) Melby, T., Despirito, M., Demasi, R., Heilek-Snyder, G., Greenberg, M. L., and Graham, N. (2006) HIV-1 Coreceptor Use in Triple-Class Treatment-Experienced Patients: Baseline Prevalence,

Correlates, and Relationship to Enfuvirtide Response. *J. Infect. Dis. 194* (2), 238−246.
(57) Wilkin, T. J., Lalama, C. M., McKinnon, J., Gandhi, R. T., Lin, N., Landay, A., Ribaudo, H., Fox, L., Currier, J. S., Mellors, J. W., Gulick, R., and Tenorio, A. R. (2012) A Pilot Trial of Adding Maraviroc to Suppressive Antiretroviral Therapy for Suboptimal CD4(+) T-Cell Recovery despite Sustained Virologic Suppression: ACTG A5256. *J. Infect. Dis. 206* (4), 534−542.
(58) Missé, D., Cerutti, M., Noraz, N., Jourdan, P., Favero, J., Devauchelle, G., Yssel, H., Taylor, N., and Veas, F. (1999) A CD4-Independent Interaction of Human Immunodeficiency Virus-1 Gp120 With CXCR4 Induces Their Cointernalization, Cell Signaling, and T-Cell Chemotaxis. *Blood 93* (8), 2454−2462.
(59) Balabanian, K., Harriague, J., Decrion, C., Lagane, B., Shorte, S., Baleux, F., Virelizier, J.-L., Arenzana-Seisdedos, F., and Chakrabarti, L. A. (2004) CXCR4-Tropic HIV-1 Envelope Glycoprotein Functions as a Viral Chemokine in Unstimulated Primary CD4+ T Lymphocytes. *J. Immunol. 173* (12), 7150−7160.
(60) Hendrix, C. W., Collier, A. C., Lederman, M. M., Schols, D., Pollard, R. B., Brown, S., Jackson, J. B., Coombs, R. W., Glesby, M. J., Flexner, C. W., Bridger, G. J., Badel, K., MacFarland, R. T., Henson, G. W., and Calandra, G. (2004) Safety, Pharmacokinetics, and Antiviral Activity of AMD3100, a Selective CXCR4 Receptor Inhibitor, in HIV-1 Infection. *JAIDS, J. Acquired Immune Defic. Syndr. 37* (2), 1253−1262.
(61) Henrich, T. J., and Kuritzkes, D. R. (2013) HIV-1 Entry Inhibitors: Recent Development and Clinical Use. *Curr. Opin. Virol. 3* (1), 51−57.
(62) Martin, C., Bridger, G. J., and Rankin, S. M. (2006) Structural Analogues of AMD3100 Mobilise Haematopoietic Progenitor Cells from Bone Marrow in Vivo According to Their Ability to Inhibit CXCL12 Binding to CXCR4 in Vitro. *Br. J. Haematol. 134* (3), 326−329.
(63) Pulliam, A. C., Hobson, M. J., Ciccone, S. L., Li, Y., Chen, S., Srour, E. F., Yang, F.-C., Broxmeyer, H. E., and Clapp, D. W. (2008) AMD3100 Synergizes with G-CSF to Mobilize Repopulating Stem Cells in Fanconi Anemia Knockout Mice. *Exp. Hematol. 36* (9), 1084−1090.
(64) Geminder, H., Sagi-Assif, O., Goldberg, L., Meshel, T., Rechavi, G., Witz, I. P., and Ben-Baruch, A. A. (2001) Possible Role for CXCR4 and Its Ligand, the CXC Chemokine Stromal Cell-Derived Factor-1, in the Development of Bone Marrow Metastases in Neuroblastoma. *J. Immunol. 167* (8), 4747−4757.
(65) Kijima, T., Maulik, G., Ma, P. C., Tibaldi, E. V., Turner, R. E., Rollins, B., Sattler, M., Johnson, B. E., and Salgia, R. (2002) Regulation of Cellular Proliferation, Cytoskeletal Function, and Signal Transduction through CXCR4 and c-Kit in Small Cell Lung Cancer Cells. *Cancer Res. 62* (21), 6304−6311.
(66) Hwang, J. H., Hwang, J. H., Chung, H. K., Kim, D. W., Hwang, E. S., Suh, J. M., Kim, H., You, K. H., Kwon, O. Y., Ro, H. K., Jo, D. Y., and Shong, M. (2003) CXC Chemokine Receptor 4 Expression and Function in Human Anaplastic Thyroid Cancer Cells. *J. Clin. Endocrinol. Metab. 88* (1), 408−416.
(67) Darash-Yahana, M., Pikarsky, E., Abramovitch, R., Zeira, E., Pal, B., Karplus, R., Beider, K., Avniel, S., Kasem, S., Galun, E., and Peled, A. (2004) Role of High Expression Levels of CXCR4 in Tumor Growth, Vascularization, and Metastasis. *FASEB J. 18* (11), 1240−1242.
(68) Schimanski, C. C., Bahre, R., Gockel, I., Muller, A., Frerichs, K., Horner, V., Teufel, A., Simiantonaki, N., Biesterfeld, S., Wehler, T., Schuler, M., Achenbach, T., Junginger, T., Galle, P. R., and Moehler, M. (2006) Dissemination of Hepatocellular Carcinoma Is Mediated via Chemokine Receptor CXCR4. *Br. J. Cancer 95* (2), 210−217.
(69) Xu, C., Zhao, H., Chen, H., and Yao, Q. (2015) CXCR4 in Breast Cancer: Oncogenic Role and Therapeutic Targeting. *Drug Des., Dev. Ther. 9*, 4953−4964.
(70) Kircher, M., Herhaus, P., Schottelius, M., Buck, A. K., Werner, R. A., Wester, H.-J., Keller, U., and Lapa, C. (2018) CXCR4-Directed Theranostics in Oncology and Inflammation. *Ann. Nucl. Med. 32* (8), 503−511.
(71) Vagima, Y., Lapid, K., Kollet, O., Goichberg, P., Alon, R., and Lapidot, T. (2011) Pathways Implicated in Stem Cell Migration: The SDF-1/CXCR4 Axis. *Methods Mol. Biol. 750*, 277−289.
(72) Launay, O., Paul, S., Servettaz, A., Roguet, G., Rozenberg, F., Lucht, F., Lambert, C., Presles, E., Goulvestre, C., Meritet, J.-F., Galtier, F., Dubray, C., Lebon, P., Weill, B., and Batteux, F. (2013) Control of Humoral Immunity and Auto-Immunity by the CXCR4/CXCL12 Axis in Lupus Patients Following Influenza Vaccine. *Vaccine 31* (35), 3492−3501.
(73) Debnath, B., Xu, S., Grande, F., Garofalo, A., and Neamati, N. (2013) Small Molecule Inhibitors of CXCR4. *Theranostics 3* (1), 47−75.
(74) Nagafuchi, Y., Shoda, H., Sumitomo, S., Nakachi, S., Kato, R., Tsuchida, Y., Tsuchiya, H., Sakurai, K., Hanata, N., Tateishi, S., Kanda, H., Ishigaki, K., Okada, Y., Suzuki, A., Kochi, Y., Fujio, K., and Yamamoto, K. (2016) Immunophenotyping of Rheumatoid Arthritis Reveals a Linkage between HLA-DRB1 Genotype, CXCR4 Expression on Memory CD4(+) T Cells, and Disease Activity. *Sci. Rep. 6*, 29338.
(75) Galkina, E., and Ley, K. (2009) Immune and Inflammatory Mechanisms of Atherosclerosis (*). *Annu. Rev. Immunol. 27*, 165−197.
(76) Bonham, L. W., Karch, C. M., Fan, C. C., Tan, C., Geier, E. G., Wang, Y., Wen, N., Broce, I. J., Li, Y., Barkovich, M. J., Yokoyama, J. S., Desikan, R. S., et al. (2018) International FTD-Genomics Consortium (IFGC); International Parkinson's Disease Genetics Consortium (IPDGC); International Genomics of Alzheimer's Project (IGAP). CXCR4 Involvement in Neurodegenerative Diseases. *Transl. Psychiatry 8* (1), 73.
(77) Conley-LaComb, M. K., Semaan, L., Singareddy, R., Li, Y., Heath, E. I., Kim, S., Cher, M. L., and Chinni, S. R. (2016) Pharmacological Targeting of CXCL12/CXCR4 Signaling in Prostate Cancer Bone Metastasis. *Mol. Cancer 15* (1), 68.
(78) Burger, M., Glodek, A., Hartmann, T., Schmitt-Graff, A., Silberstein, L. E., Fujii, N., Kipps, T. J., and Burger, J. A. (2003) Functional Expression of CXCR4 (CD184) on Small-Cell Lung Cancer Cells Mediates Migration, Integrin Activation, and Adhesion to Stromal Cells. *Oncogene 22* (50), 8093−8101.
(79) Kim, J., Takeuchi, H., Lam, S. T., Turner, R. R., Wang, H. J., Kuo, C., Foshag, L., Bilchik, A. J., and Hoon, D. S. B. (2005) Chemokine Receptor CXCR4 Expression in Colorectal Cancer Patients Increases the Risk for Recurrence and for Poor Survival. *J. Clin. Oncol. 23* (12), 2744−2753.
(80) Ehtesham, M., Mapara, K. Y., Stevenson, C. B., and Thompson, R. C. (2009) CXCR4Mediates the Proliferation of Glioblastoma Progenitor Cells. *Cancer Lett. 274* (2), 305−312.
(81) Scasnár, V., and van Lier, J. E. (1993) The Use of SEP-PAK SI Cartridges for the Preparation of Gallium Chloride from the Citrate Solution. *Eur. J. Nucl. Med. 20*, 273.
(82) Wu, L., Martin, T. D., Carrington, M., and KewalRamani, V. N. (2004) Raji B Cells, Misidentified as THP-1 Cells, Stimulate DC-SIGN-Mediated HIV Transmission. *Virology 318* (1), 17−23.
(83) Amara, A., Vidy, A., Boulla, G., Mollier, K., Garcia-Perez, J., Alcamí, J., Blanpain, C., Parmentier, M., Virelizier, J.-L., Charneau, P., and Arenzana-Seisdedos, F. (2003) G Protein-Dependent CCR5 Signaling Is Not Required for Efficient Infection of Primary T Lymphocytes and Macrophages by R5 Human Immunodeficiency Virus Type 1 Isolates. *J. Virol. 77* (4), 2550−2558.
(84) Zhang, H., Zhou, Y., Alcock, C., Kiefer, T., Monie, D., Siliciano, J., Li, Q., Pham, P., Cofrancesco, J., Persaud, D., and Siliciano, R. F. (2004) Novel Single-Cell-Level Phenotypic Assay for Residual Drug Susceptibility and Reduced Replication Capacity of Drug-Resistant Human Immunodeficiency Virus Type 1. *J. Virol. 78* (4), 1718−1729.
(85) Chang, L. J., Urlacher, V., Iwakuma, T., Cui, Y., and Zucali, J. (1999) Efficacy and Safety Analyses of a Recombinant Human Immunodeficiency Virus Type 1 Derived Vector System. *Gene Ther. 6* (5), 715−728.

https://dx.doi.org/10.1021/acsinfecdis.9b00507
ACS Infect. Dis. 2021, 7, 6−22

(86) Rato, S., Maia, S., Brito, P. M., Resende, L., Pereira, C. F., Moita, C., Freitas, R. P., Moniz-Pereira, J., Hacohen, N., Moita, L. F., and Goncalves, J. (2010) Novel HIV-1 Knockdown Targets Identified by an Enriched Kinases/Phosphatases ShRNA Library Using a Long-Term Iterative Screen in Jurkat T-Cells. *PLoS One 5* (2), e9276.
(87) Kwon, M., and Firestein, B. L. (2013) DNA Transfection: Calcium Phosphate Method. *Methods Mol. Biol. 1018*, 107−110.
(88) Reed, L. J., and Muench, H. (1938) A Simple Method of Estimating Fifty per Cent Endpoints. *Am. J. Epidemiol. 27* (3), 493−497.
(89) Wood, K. V. (1990) Luc Genes: Introduction of Colour into Bioluminescence Assays. *J. Biolumin. Chemilumin. 5* (2), 107−114.
(90) Montefiori, D. C. (2009) Measuring HIV Neutralization in a Luciferase Reporter Gene Assay. *Methods Mol. Biol. 485*, 395−405.
(91) Freed, E. O., Englund, G., and Martin, M. A. (1995) Role of the Basic Domain of Human Immunodeficiency Virus Type 1 Matrix in Macrophage Infection. *J. Virol. 69* (6), 3949−3954.
(92) Lu, J., Sista, P., Giguel, F., Greenberg, M., and Kuritzkes, D. R. (2004) Relative Replicative Fitness of Human Immunodeficiency Virus Type 1 Mutants Resistant to Enfuvirtide (T-20). *J. Virol. 78* (9), 4628−4637.
(93) Borrego, P., Calado, R., Marcelino, J. M., Bartolo, I., Rocha, C., Cavaco-Silva, P., Doroana, M., Antunes, F., Maltez, F., Caixas, U., Barroso, H., and Taveira, N. (2012) Baseline Susceptibility of Primary HIV-2 to Entry Inhibitors. *Antiviral Ther. 17* (3), 565−570.
(94) Chou, T. C. (1976) Derivation and Properties of Michaelis-Menten Type and Hill Type Equations for Reference Ligands. *J. Theor. Biol. 59* (2), 253−276.
(95) National Research Council of the National Academies (2011) *Guide for the Care and Use of Laboratory Animals*, 8th ed., National Academies Press, Washington, DC.
(96) Toohey, K., Wehrly, K., Nishio, J., Perryman, S., and Chesebro, B. (1995) Human Immunodeficiency Virus Envelope V1 and V2 Regions Influence Replication Efficiency in Macrophages by Affecting Virus Spread. *Virology 213* (1), 70−79.
(97) Wehrly, K., and Chesebro, B. (1997) P24 Antigen Capture Assay for Quantification of Human Immunodeficiency Virus Using Readily Available Inexpensive Reagents. *Methods 12* (4), 288−293.
(98) Princen, K., Hatse, S., Vermeire, K., De Clercq, E., and Schols, D. (2003) Evaluation of SDF-1/CXCR4-Induced Ca2+ Signaling by Fluorometric Imaging Plate Reader (FLIPR) and Flow Cytometry. *Cytometry 51A* (1), 35−45.
(99) Gee, K. R., Brown, K. A., Chen, W. N. U., Bishop-Stewart, J., Gray, D., and Johnson, I. (2000) Chemical and Physiological Characterization of Fluo-4 Ca2+-Indicator Dyes. *Cell Calcium 27* (2), 97−106.

https://dx.doi.org/10.1021/acsinfecdis.9b00507
ACS Infect. Dis. 2021, 7, 6−22